Published by Institute of Physics Publishing for SISSA/ISAS
Received: *October 4, 2004*
Revised: *February 11, 2005*
Accepted: *February 11, 2005*

Deeply virtual neutrino scattering (DVNS)

Paolo Amore,[a] **Claudio Corianò**[bc] **and Marco Guzzi**[b]

[a] *Facultad de Ciencias, Universidad de Colima*
Av. 25 de Julio 965, Colima Colima, 28045 Mexico
[b] *Dipartimento di Fisica, Università di Lecce and INFN Sezione di Lecce*
Via Arnesano 73100 Lecce, Italy
[c] *Department of Physics and Institute of Plasma Physics*
University of Crete and FORTH, Heraklion, Greece
E-mail: paolo@ucol.mx, claudio.coriano@le.infn.it, marco.guzzi@le.infn.it

Abstract: We introduce the study of neutrino scattering off protons in the deeply virtual kinematics, which describes under a unified formalism elastic and deep inelastic neutrino scattering. A real final state photon and a recoiling nucleon are detected in the few GeV ($|t| \sim 0.2 - 5\,\mathrm{GeV}$) region of momentum transfer. This is performed via an extension of the notion of deeply virtual Compton scattering, or DVCS, to the case of a neutral current exchange. The relevance of this process and of other similar exclusive processes for the study of neutrino interactions in neutrino factories for GeV neutrinos is pointed out.

Keywords: QCD, Parton Model.

Contents

1. Introduction

There is no doubt that the study of neutrino masses and of flavour mixing in the leptonic sector will play a crucial role for uncovering new physics beyond the Standard Model and to test Unification. In fact, the recent discovery of neutrino oscillations in atmospheric and solar neutrinos (see [1] for an overview) has raised the puzzle of the origin of the mass hierarchy among the various neutrino flavours, a mystery which, at the moment, remains unsolved. The study of the mixing among the leptons also raises the possibility of detecting possible sources of CP violation in this sector as well. It seems then obvious that the study of these aspects of flavour physics requires the exploration of a new energy range for neutrino production and detection beyond the one which is accessible at this time.

For this purpose, several proposals have been presented recently for neutrino factories, where a beam, primarily made of muon neutrinos produced at an accelerator facility, is directed to a large volume located several hundreds kilometers away at a second facility. The goal of these experimental efforts is to uncover various possible patterns of mixings among flavours - using the large distance between the points at which neutrinos are produced and detected - in order to study in a more detailed and "artificial" way the phenomenon of oscillations. Detecting neutrinos at this higher energies is an aspect that deserves special attention since several of these experimental proposals [2, 3, 4] require a nominal energy of the neutrino beam in the few GeV region. We recall that the incoming neutrino beam, scattering off deuteron or other heavier targets at the detector facility, has an energy which covers, in the various proposals, both the resonant, the quasi-elastic (in the GeV range) and the deep inelastic region (DIS) at higher energy. In the past, neutrino scattering on nucleons has been observed over a wide interval of energy, ranging from few MeV up to 100 GeV, and these studies have been of significant help for uncovering the structure of the fundamental interactions in the Standard Model. Generally, one envisions contributions to the scattering cross section either in the low energy region, such as in neutrino-nucleon elastic scattering, or in the deep inelastic scattering (DIS) region. Recent developments in perturbative QCD have emphasized that exclusive (see [5]) and inclusive processes can be unified under a general treatment using a factorization approach in a generalized kinematical domain. The study of this domain, termed deeply virtual Compton scattering, or DVCS, is an area of investigation of wide theoretical interest, with experiments planned in the next few years at JLAB and at DESY. The key constructs of the DVCS domain are the non-forward parton distributions, where the term *non-forward* is there to indicate the asymmetry between the initial and final state typical of a true Compton process, in this case appearing not through unitarity, such as in DIS, but at amplitude level.

In this work, after a brief summary of the generalities of process, we discuss its generalization to the case of neutral currents. We recall that DVCS has been extensively studied in the last few years for electromagnetic interactions. The extension of DVCS to the case of neutral currents is presented here, while the charged current version will be presented in a forthcoming paper. Also, in this work we will just focus on the lowest order contributions to the process, named by us Deeply Virtual Neutrino Scattering (DVNS) in order to distinguish it from standard DVCS, while a renormalization group analysis of the factorized amplitude, which requires an inclusion of the modifications induced by the evolution will also be presented elsewhere. The application of the formalism that we develop here also needs a separate study of the isoscalar cross sections together with a detailed analysis of the various experimental constraints at neutrino factories in order to be applicable at forthcoming experiments.

2. The generalized Bjorken region and DVCS

Compton scattering has been investigated in the near past by several groups, since the original work by Ji and Radyushkin [6, 7, 8]. Previous work on the generalized Bjorken region, which includes DVCS and predates the "DVCS period" can be found in [9].

A pictorial description of the process we are going to illustrate is given in figure 1 where a neutrino of momentum l scatters off a nucleon of momentum P_1 by an interaction with a neutral current; from the final state a photon and a nucleon emerge, of momenta q_2 and P_2 respectively, while the momenta of the final lepton is l'. The process is described

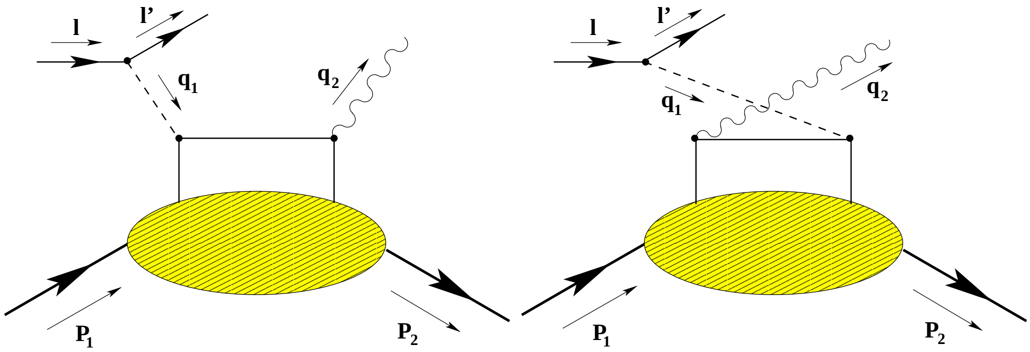

Figure 1: Leading hand-bag diagrams for the process.

in terms of new constructs of the parton model termed generalized parton distributions (GPD) or also non-forward (off-forward) parton distributions. We recall that the regime for the study of GPD's is characterized by a deep virtuality of the exchanged photon in the initial interaction $(e+p \to e+p+\gamma)$ ($Q^2 \approx 2\,\mathrm{GeV}^2$), with the final state photon kept on-shell; large energy of the hadronic system ($W^2 > 6\,\mathrm{GeV}^2$) above the resonance domain and small momentum transfers $|t| < 1\,\mathrm{GeV}^2$. The process suffers of a severe Bethe-Heitler (BH) background, with photon emission taking place from the lepton. Therefore, in the relevant region, characterized by large Q^2 and small t, the dominant Bethe-Heitler background ($\sim 1/t$) and the $1/Q$ behaviour of the DVCS scattering amplitude render the analysis quite complex. From the experimental viewpoint a dedicated study of the interference BH-VCS is required in order to explore the generalized Bjorken region, and this is done by measuring asymmetries. Opting for a symmetric choice for the defining momenta, we use as independent variables the average of the hadron and gauge bosons momenta

$$P_{1,2} = \bar{P} \pm \frac{\Delta}{2} \qquad q_{1,2} = \bar{q} \mp \frac{\Delta}{2} \tag{2.1}$$

with $-\Delta = P_2 - P_1$ being the momentum transfer. Clearly

$$\bar{P} \cdot \Delta = 0\,, \qquad t = \Delta^2 \qquad \bar{P}^2 = M^2 - \frac{t}{4} \tag{2.2}$$

and M is the nucleon mass. There are two scaling variables which are identified in the process, since 3 scalar products can grow large in the generalized Bjorken limit: $\bar{q}^2$, $\Delta \cdot q$, $\bar{P} \cdot \bar{q}$.

The momentum transfer $t = \Delta^2$ is a small parameter in the process. Momentum asymmetries between the initial and the final state nucleon are measured by two scaling parameters, ξ and η, related to ratios of the former invariants

$$\xi = -\frac{\bar{q}^2}{2\bar{P} \cdot \bar{q}} \qquad \eta = \frac{\Delta \cdot \bar{q}}{2\bar{P} \cdot \bar{q}} \tag{2.3}$$

where ξ is a variable of Bjorken type, expressed in terms of average momenta rather than nucleon and Z-boson momenta. The standard Bjorken variable $x = -q_1^2/(2P_1 \cdot q_1)$ is trivially related to ξ in the $t = 0$ limit. In the DIS limit ($P_1 = P_2$) $\eta = 0$ and $x = \xi$, while in the DVCS limit $\eta = \xi$ and $x = 2\xi/(1+\xi)$, as one can easily deduce from the relations

$$q_1^2 = \left(1 + \frac{\eta}{\xi}\right)\bar{q}^2 + \frac{t}{4}, \qquad q_2^2 = \left(1 - \frac{\eta}{\xi}\right)\bar{q}^2 + \frac{t}{4}. \tag{2.4}$$

We introduce also the inelasticity parameter $y = P_1 \cdot l/(P_1 \cdot q_1)$ which measures the fraction of the total energy that is transferred to the final state photon. Notice also that $\xi = \frac{\Delta^+}{2\bar{P}^+}$ measures the ratio between the plus component of the momentum transfer and the average momentum. A second scaling variable, related to ξ is $\zeta = \Delta^+/{P_1}^+$, which coincides with Bjorken x ($x = \zeta$) when $t = 0$.

ξ, therefore, parametrizes the large component of the momentum transfer Δ, which can be generically described as

$$\Delta = 2\xi\bar{P} + \hat{\Delta} \tag{2.5}$$

where all the components of $\hat{\Delta}$ are $O(\sqrt{t})$ [10].

3. DIS versus DVNS

In the study of ordinary DIS scattering of neutrinos on nucleons (see figure 2), the relevant current correlator is obtained from the T-product of two neutral currents acting on a forward nucleon state of momentum P_1

$$j_Z^\mu \equiv \overline{u}(l')\gamma^\mu\left(-1 + 4\sin^2\theta_W + \gamma_5\right)u(l) \tag{3.1}$$

where θ_W is the Weinberg angle, l and l' are the initial and final-state lepton. The relevant correlator is given by

$$T_{\mu\nu}(q_1^2, \nu) = i\int d^4z e^{iq\cdot z}\langle P_1|T(J_Z^\mu(\xi)J_Z^\nu(0)|P_1\rangle \tag{3.2}$$

with $\nu = E - E'$ being the energy transfered to the nucleon, P_1 is the initial-state nucleon 4-momenta and $q_1 = l - l'$ is the momentum transfered. The hadronic tensor $W_{\mu\nu}$ is related to the imaginary part of this correlator by the optical theorem. We recall that for an inclusive

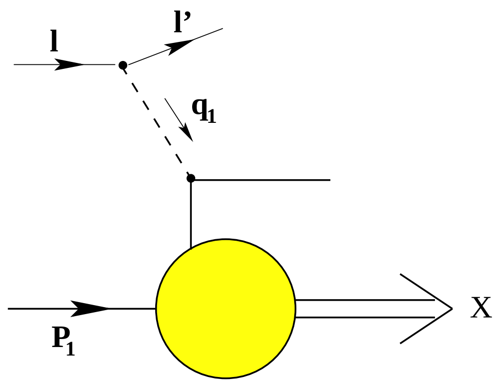

Figure 2: Leading diagram for a generic DIS process.

electroweak process mediated by neutral currents the hadronic tensor (for unpolarized scatterings) is identified in terms of 3 independent structure functions at leading twist

$$W_{\mu\nu} = \left(-g_{\mu\nu} + \frac{q_{1\mu}q_{1\nu}}{q_1^2}\right) W_1(\nu, Q^2) + \frac{\hat{P_1}^{\mu}\hat{P_1}^{\nu}}{P_1^2}\frac{W_2(\nu, Q^2)}{M^2} - i\epsilon_{\mu\nu\lambda\sigma}q_1^{\lambda}P_1^{\sigma}\frac{W_3(\nu, Q^2)}{2M^2} \tag{3.3}$$

where transversality of the current is obvious since $\hat{P_1}^{\mu} = P_1^{\mu} - q_1^{\mu}P_1 \cdot q_1/q_1^2$.

The analysis at higher twists is far more involved and the total number of structure functions appearing is 14 if we include polarization effects. These are fixed by the requirements of Lorenz covariance and time reversal invariance, neglecting small CP-violating effects from the CKM matrix. Their number can be reduced to 8 if current conservation is imposed, which is equivalent to requiring that contributions proportional to non-vanishing current quark masses can be dropped (see also [11]). We recall that the DIS limit is performed by the identifications

$$\begin{aligned} MW_1(Q^2, \nu) &= F_1(x, Q^2) \\ \nu W_2(Q^2, \nu) &= F_2(x, Q^2) \\ \nu W_3(Q^2, \nu) &= F_3(x, Q^2)\,, \end{aligned} \tag{3.4}$$

in terms of the standard structure functions F_1, F_2 and F_3. There are various ways to express the neutrino-nucleon DIS cross section, either in terms of Q^2 and the energy transfer, in which the scattering angle θ is integrated over, or as a triple cross section in (Q^2, ν, θ), or yet in terms of the Bjorken variable x, inelasticity y and the scattering angle (x, y, θ). This last case is close to the kinematical setup of our study. In this case the differential Born cross section in DIS is given by

$$\frac{d^3\sigma}{dx dy d\theta} = \frac{y\alpha^2}{Q^4}\sum_i \eta_i(Q^2) L_i^{\mu\nu} W_i^{\mu\nu}\,, \tag{3.5}$$

the index i denotes the different current contributions, ($i = |\gamma|^2, |\gamma Z|, |Z|^2$ for the neutral current) and α denotes the fine structure constant. By θ we indicate the azimuthal angle of the final-state lepton, while $y = (P_1 \cdot q_1)/(l \cdot P_1)$ is the inelasticity parameter, and $Q^2 = -q_1^2$. The factors $\eta_i(Q^2)$ denote the ratios of the corresponding propagator terms to the photon propagator squared,

$$\begin{aligned} \eta^{|\gamma|^2}(Q^2) &= 1\,, \\ \eta^{|\gamma Z|}(Q^2) &= \frac{G_F M_Z^2}{2\sqrt{2}\pi\alpha}\frac{Q^2}{Q^2 + M_Z^2}\,, \\ \eta^{|Z|^2}(Q^2) &= (\eta^{|\gamma Z|})^2(Q^2)\,. \end{aligned} \tag{3.6}$$

where G_F is the Fermi constant and M_Z is the mass of the Z boson while the leptonic tensor has the form

$$L^i_{\mu\nu} = \sum_{\lambda'}\left[\bar{u}(k', \lambda')\gamma_\mu(g_V^{i_1} + g_A^{i_1}\gamma_5)u(k, \lambda)\right]^* \bar{u}(k', \lambda')\gamma_\nu(g_V^{i_2} + g_A^{i_2}\gamma_5)u(k, \lambda)\,. \tag{3.7}$$

In the expression above λ and λ', denote the initial and final-state helicity of the leptons. The indices i_1 and i_2 refer to the sum appearing in eq. (3.5)

$$\begin{aligned} g_V^\gamma &= 1\,, & g_A^\gamma &= 0\,, \\ g_V^Z &= -\frac{1}{2} + 2\sin^2\theta_W\,, & g_A^Z &= \frac{1}{2}\,, \end{aligned} \tag{3.8}$$

In the case of neutrino/nucleon interaction mediated by the neutral current the dominant diagram for this process appears in figure 2. A similar diagram, with the obvious modifications, describes also charged current exchanges. We recall that the unpolarized cross section is expressed in terms of F_1 and F_2, since F_3 disappears in this special case, and in particular, after an integration over the scattering angle of the final state neutrino one obtains

$$\frac{d^2\sigma}{dxdy} = 2\pi S\frac{\alpha^2}{Q^4}(g_V^Z)^2\eta^{|\gamma Z|}(Q^2)\left(2xy^2F_1 + 2\left(1 - x - \frac{xyM^2}{S}\right)F_2\right), \tag{3.9}$$

where $S = 2ME_\nu$ is the nucleon-neutrino center of mass energy.

We also recall that in this case the cross section in the parton model is given by

$$\frac{d^2\sigma}{dxdy} = \frac{G_F^2 ME_\nu}{2\pi}\left(\frac{M_Z^2}{Q^2+M_Z^2}\right)^2\left[xq^0(x,Q^2) + x\bar{q}^0(x,Q^2)(1-y)^2\right] \tag{3.10}$$

where $q^0(x,Q^2)$ and $\bar{q}^0(x,Q^2)$ are linear combinations of parton distributions

$$\begin{aligned} q^0(x,Q^2) &= \left[\frac{u_v(x,Q^2)+d_v(x,Q^2)}{2} + \frac{\bar{u}(x,Q^2)+\bar{d}(x,Q^2)}{2}\right](L_u^2+L_d^2) + \\ &\quad + \left[\frac{\bar{u}(x,Q^2)+\bar{d}(x,Q^2)}{2}\right](R_u^2+R_d^2) \\ \bar{q}^0(x,Q^2) &= \left[\frac{u_v(x,Q^2)+d_v(x,Q^2)}{2} + \frac{\bar{u}(x,Q^2)+\bar{d}(x,Q^2)}{2}\right](R_u^2+R_d^2) + \\ &\quad + \left[\frac{\bar{u}(x,Q^2)+\bar{d}(x,Q^2)}{2}\right](L_u^2+L_d^2) \end{aligned} \tag{3.11}$$

with

$$\begin{aligned} L_u &= 1 - \frac{4}{3}\sin^2\theta_W\,, & L_d &= -1 + \frac{2}{3}\sin^2\theta_W \\ R_u &= -\frac{4}{3}\sin^2\theta_W\,, & R_d &= \frac{2}{3}\sin^2\theta_W \end{aligned} \tag{3.12}$$

and we have identified the sea contributions u_s and d_s with $\bar{u}$ and $\bar{d}$ rispectively.

Let's now move to the nonforward case. Here, when a real photon is present in the final state, the relevant correlator is given by

$$T_{\mu\nu}(q_1^2,\nu) = i\int d^4z e^{iq\cdot z}\left\langle \bar{P} - \frac{\Delta}{2}\right|T\left(J_Z^\mu\left(-\frac{z}{2}\right)J_\gamma^\nu\left(\frac{z}{2}\right)\left|\bar{P} + \frac{\Delta}{2}\right\rangle\right.. \tag{3.13}$$

The dominant diagrams for this process appears in figure 1. We impose Ward identities on both indices, which is equivalent to requiring that terms proportional to the quark masses in $\partial \cdot J_Z$ are neglected. This approximation is analogous to the one performed in

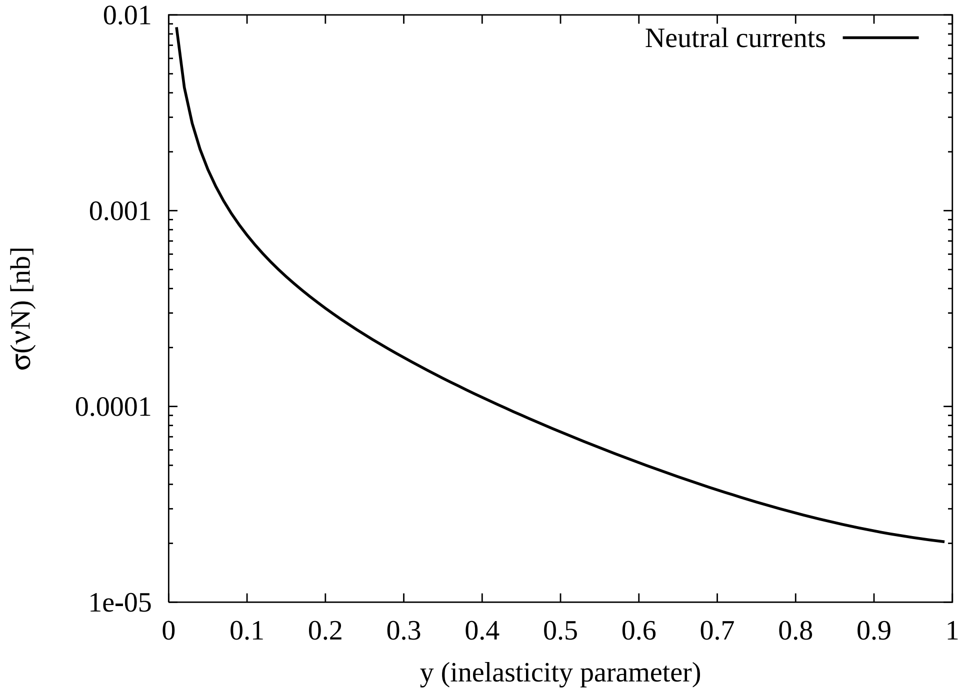

Figure 3: The cross section of a neutrino process of DIS-type at $x \approx 0.1$ with neutral current at ultrahigh energy.

the forward case in order to reduce the structure functions from 8 to 3 (in the absence of any polarization), imposing symmetric trasversality conditions on the weak currents

$$\left(\bar{P}^{\mu} - \frac{\Delta^{\mu}}{2}\right) T_{\mu\nu} = 0 \qquad \left(\bar{P}^{\mu} + \frac{\Delta^{\mu}}{2}\right) T_{\mu\nu} = 0\,. \tag{3.14}$$

The leading twist contribution to DVNS is obtained by performing a collinear expansion of the loop momentum of the hand-bag diagram and neglecting terms of order $O(\Delta_{\perp}^2/Q^2)$ and M^2/Q^2. Transversality is satisfied at this order. Violation of transversality condition in the hand-bag approximation is analogous to the DVCS case, where it has been pointed out that one has to include systematically “kinematical” twist-3 operators, which appear as total derivatives of twist-2 operators [10, 12] in order to restore it.

For the parametrization of the hand-bag diagram (figure 1) we use the light-cone decomposition in terms of 2 four-vectors $(n, \tilde{n})$, where

$$\begin{aligned}
\tilde{n}^{\mu} &= \Lambda(1,0,0,1) \\
n^{\mu} &= \frac{1}{2\Lambda}(1,0,0,-1) \\
\tilde{n}^2 &= n^2 = 0\,, \qquad \tilde{n}\cdot n = 1\,.
\end{aligned}$$

At the same time we set

$$\begin{aligned}
P_1^{\mu} &= (1+\xi)\tilde{n}^{\mu} + (1-\xi)\frac{\overline{M}}{2}n^{\mu} - \frac{\Delta_{\perp}^{\mu}}{2} \\
P_2^{\mu} &= (1+\xi)\tilde{n}^{\mu} + (1+\xi)\frac{\overline{M}}{2}n^{\mu} + \frac{\Delta_{\perp}^{\mu}}{2}
\end{aligned}$$

$$
\begin{aligned}
q_1^\mu &= -2\xi\tilde{n}^\mu + \frac{Q^2}{4\xi}n^\mu \\
k^\mu &= (k\cdot n)\,\tilde{n}^\mu + (k\cdot\tilde{n})\,n^\mu + k_\perp^\mu \\
\overline{M}^2 &= M^2 - \frac{\Delta^2}{4}
\end{aligned}
\tag{3.15}
$$

with $\bar{P}^2 = \overline{M}^2$. We will also use the notation $-q_1^2 = Q^2$ for the invariant mass of the virtual Z boson and we will denote by $\bar{q}$ the average gauge bosons momenta respectively.

After a collinear expansion of the loop momentum we obtain

$$
\begin{aligned}
T_A^{\mu\nu} &= i\int\frac{d^4k}{(2\pi)^4}\,\mathrm{tr}\left\{g_u\gamma^\nu \not{P}_D\gamma^\mu\tilde{g}\left(U_v-\gamma^5\right)\underline{M}^u(k) + g_d\gamma^\nu \not{P}_D\gamma^\mu\tilde{g}\left(D_v-\gamma^5\right)\underline{M}^d(k)\right\} \\
T_B^{\mu\nu} &= i\int\frac{d^4k}{(2\pi)^4}\,\mathrm{tr}\left\{\tilde{g}\gamma^\mu\left(U_v-\gamma^5\right)\not{P}_E\gamma^\nu g_u\underline{M}^u(k) + \tilde{g}\gamma^\mu\left(D_v-\gamma^5\right)\not{P}_E\gamma^\nu g_d\underline{M}^d(k)\right\}
\end{aligned}
\tag{3.16}
$$

where we have used the following notations

$$
\begin{aligned}
g_u &= \frac{2}{3}e\,, \qquad g_d = \frac{1}{3}e\,, \qquad \tilde{g} = \frac{g}{4\cos\left(\theta_W\right)}\,, \\
U_v &= 1-\frac{8}{3}\sin^2\theta_W\,, \qquad D_v = 1-\frac{4}{3}\sin^2\theta_W\,,
\end{aligned}
\tag{3.17}
$$

$$
\begin{aligned}
\not{P}_D &= \frac{\not{k} - \alpha\not{\Delta} + \not{q}_1}{\left(k-\alpha\Delta+q_1\right)^2+i\epsilon}\,, \\
\not{P}_E &= \frac{\not{k} - \not{q}_1 + \not{\Delta}\,(1-\alpha)}{\left(k-q_1+\Delta(1-\alpha)\right)^2+i\epsilon}
\end{aligned}
\tag{3.18}
$$

where the constant α (α is a free parameter) ranges between 0 and 1. The $\underline{M}$ matrix is the quark density matrix and is given by

$$
\underline{M}_{ab}^{(i)}(k) = \int d^4y e^{ik\cdot y}\langle P'|\overline{\psi}_a^{(i)}(-\alpha y)\psi_b^{(i)}((1-\alpha)y)|P\rangle\,. \tag{3.19}
$$

The index $i = u,d$ runs on flavours. Using a Sudakov decomposition of the internal loop we can rewrite $T_A^{\mu\nu}$ and $T_B^{\mu\nu}$ as

$$
\begin{aligned}
T_A^{\mu\nu} &= i\int\frac{d(k\cdot n)}{(2\pi)^4}d(k\cdot\tilde{n})d^2k_\perp\int\frac{d\lambda}{(2\pi)}dz e^{i\lambda(z-k\cdot n)}\times \\
&\times\mathrm{tr}\left\{g_u\gamma^\nu \not{P}_D\gamma^\mu\tilde{g}\left(U_v-\gamma^5\right)\underline{M}^u(k) + g_d\gamma^\nu \not{P}_D\gamma^\mu\tilde{g}\left(D_v-\gamma^5\right)\underline{M}^d(k)\right\} \\
T_B^{\mu\nu} &= i\int\frac{d(k\cdot n)}{(2\pi)^4}d(k\cdot\tilde{n})d^2k_\perp\int\frac{d\lambda}{(2\pi)}dz e^{i\lambda(z-k\cdot n)}\times \\
&\times\mathrm{tr}\left\{\tilde{g}\gamma^\mu\left(U_v-\gamma^5\right)\not{P}_E\gamma^\nu g_u\underline{M}^u(k) + \tilde{g}\gamma^\mu\left(D_v-\gamma^5\right)\not{P}_E\gamma^\nu g_d\underline{M}^d(k)\right\}
\end{aligned}
\tag{3.20}
$$

to which we will refer as the direct and the exchange diagram respectively. It is also convenient to introduce two new linear combinations $T^{\mu\nu} = T_A^{\mu\nu} + T_B^{\mu\nu} = \tilde{T}_A^{\mu\nu} + \tilde{T}_B^{\mu\nu}$ which will turn useful in order to separate Vector (V) and axial vector parts (A) of the expansion

$$\begin{aligned}
\tilde{T}_A^{\mu\nu} &= i\int \frac{d(k\cdot n)}{(2\pi)^4} d(k\cdot\tilde{n}) d^2k_\perp \int \frac{d\lambda}{(2\pi)} dz e^{i\lambda(z-k\cdot n)} \times \\
&\quad \times \tilde{g} g_u U_v \,\mathrm{tr}\left\{\left[\gamma^\nu \not{P}_D \gamma^\mu + \gamma^\mu \not{P}_E \gamma^\nu\right] \underline{M}^u(k)\right\} + \\
&\quad + \tilde{g} g_d D_v \,\mathrm{tr}\left\{\left[\gamma^\nu \not{P}_D \gamma^\mu + \gamma^\mu \not{P}_E \gamma^\nu\right] \underline{M}^d(k)\right\} \\
\tilde{T}_B^{\mu\nu} &= -i\int \frac{d(k\cdot n)}{(2\pi)^4} d(k\cdot\tilde{n}) d^2k_\perp \int \frac{d\lambda}{(2\pi)} dz e^{i\lambda(z-k\cdot n)} \times \\
&\quad \times \tilde{g} g_u \,\mathrm{tr}\left\{\left[\gamma^\nu \not{P}_D \gamma^\mu + \gamma^\mu \not{P}_E \gamma^\nu\right] \gamma^5 \underline{M}^u(k)\right\} + \\
&\quad + \tilde{g} g_d \,\mathrm{tr}\left\{\left[\gamma^\nu \not{P}_D \gamma^\mu + \gamma^\mu \not{P}_E \gamma^\nu\right] \gamma^5 \underline{M}^d(k)\right\},
\end{aligned} \tag{3.21}$$

with $\tilde{T}_A$ including the vector parts ($V\times V + A\times A$) and $\tilde{T}_B$ the axial-vector parts ($V\times A + A\times V$). After some algebraic manipulations we finally obtain

$$\begin{aligned}
\tilde{T}_A^{\mu\nu} &= \frac{i}{2}\sum_{i=u,d} \tilde{g} g_i C_i \int \frac{d\lambda dz}{(2\pi)} e^{i\lambda z}\Big\{(\tilde{n}^\mu n^\nu + \tilde{n}^\nu n^\mu - g^{\mu\nu})\alpha(z) \times \\
&\qquad \times \langle P'|\overline{\psi}^{(i)}\left(-\frac{\lambda n}{2}\right)\not{n}\ \psi^{(i)}\left(\frac{\lambda n}{2}\right)|P\rangle + i\epsilon^{\mu\nu\alpha\beta}\tilde{n}_\alpha n_\beta \beta(z) \times \\
&\qquad \times \langle P'|\overline{\psi}^{(i)}\left(-\frac{\lambda n}{2}\right)\gamma^5\not{n}\ \psi^{(i)}\left(\frac{\lambda n}{2}\right)|P\rangle\Big\} \\
\tilde{T}_B^{\mu\nu} &= -\frac{i}{2}\sum_{i=u,d} \tilde{g} g_i \int \frac{d\lambda dz}{(2\pi)} e^{i\lambda z}\Big\{(\tilde{n}^\mu n^\nu + \tilde{n}^\nu n^\mu - g^{\mu\nu})\alpha(z) \times \\
&\qquad \times \langle P'|\overline{\psi}^{(i)}\left(-\frac{\lambda n}{2}\right)\gamma^5\not{n}\ \psi^{(i)}\left(\frac{\lambda n}{2}\right)|P\rangle + \\
&\qquad + i\epsilon^{\mu\nu\alpha\beta}\tilde{n}_\alpha n_\beta \beta(z) \times \\
&\qquad \times \langle P'|\overline{\psi}^{(i)}\left(-\frac{\lambda n}{2}\right)\not{n}\ \psi^{(i)}\left(\frac{\lambda n}{2}\right)|P\rangle\Big\}
\end{aligned} \tag{3.22}$$

where $C_i = U_v,\, D_v$ and

$$\alpha(z) = \left(\frac{1}{z-\xi+i\epsilon} + \frac{1}{z+\xi-i\epsilon}\right), \qquad \beta(z) = \left(\frac{1}{z-\xi+i\epsilon} - \frac{1}{z+\xi-i\epsilon}\right) \tag{3.23}$$

are the “first order” propagators appearing in the factorization of the amplitude. We recall, if not obvious, that differently from DIS, DVCS undergoes factorization directly at amplitude level [13].

The parameterizations of the non-forward light cone correlators in terms of GPD's is of the form given by Ji at leading twist [6]

$$\begin{aligned}
&\int \frac{d\lambda}{(2\pi)} e^{i\lambda z}\langle P'|\overline{\psi}\left(-\frac{\lambda n}{2}\right)\gamma^\mu\psi\left(\frac{\lambda n}{2}\right)|P\rangle = \\
&\qquad = H(z,\xi,\Delta^2)\overline{U}(P')\gamma^\mu U(P) + E(z,\xi,\Delta^2)\overline{U}(P')\frac{i\sigma^{\mu\nu}\Delta_\nu}{2M}U(P) + \cdots
\end{aligned}$$

$$\int \frac{d\lambda}{(2\pi)} e^{i\lambda z} \langle P'|\overline{\psi}\left(-\frac{\lambda n}{2}\right)\gamma^\mu\gamma^5\psi\left(\frac{\lambda n}{2}\right)|P\rangle =$$
$$= \tilde{H}(z,\xi,\Delta^2)\overline{U}(P')\gamma^\mu\gamma^5 U(P) + \tilde{E}(z,\xi,\Delta^2)\overline{U}(P')\frac{\gamma^5\Delta^\mu}{2M}U(P) + \cdots \quad (3.24)$$

which have been expanded in terms of functions $H, E, \tilde{H}, \tilde{E}$ [14] and the ellipses are meant to denote the higher-twist contributions. It is interesting to observe that the amplitude is still described by the same light-cone correlators as in the electromagnetic case (vector, axial vector) but now parity is not conserved.

4. Operatorial analysis

The operatorial structure of the T-order product of one electroweak current and one electromagnetic current is relevant in order to identify the independent amplitudes appearing in the correlator at leading twist and the study is presented here. We will identify four operatorial structures. For this purpose let's start from the Fourier transform of the correlator of the two currents

$$T_{\mu\nu} = i\int d^4x e^{iqx}\langle P_2|T\left(J_\nu^\gamma\left(\frac{x}{2}\right)J_\mu^{Z_0}\left(-\frac{x}{2}\right)\right)|P_1\rangle\,, \quad (4.1)$$

where for the neutral and electromagnetic currents we have the following expressions

$$\begin{aligned} J^{\mu Z_0}\left(-\frac{x}{2}\right) &= \frac{g}{2\cos\theta_W}\overline{\psi}_u\left(-\frac{x}{2}\right)\gamma^\mu(g_{uV}^Z + g_{uA}^Z\gamma^5)\psi_u\left(-\frac{x}{2}\right) + \\ &\quad + \overline{\psi}_d\left(-\frac{x}{2}\right)\gamma^\mu(g_{dV}^Z + g_{dA}^Z\gamma^5)\psi_d\left(-\frac{x}{2}\right), \\ J^{\nu,\gamma}\left(\frac{x}{2}\right) &= \overline{\psi}_d\left(\frac{x}{2}\right)\gamma^\nu\left(-\frac{1}{3}e\right)\psi_d\left(\frac{x}{2}\right) + \overline{\psi}_u(x/2)\gamma^\nu\left(\frac{2}{3}e\right)\psi_u\left(\frac{x}{2}\right). \end{aligned} \quad (4.2)$$

By simple calculations one obtains

$$\begin{aligned} \langle P_2|T\left(J_\nu^\gamma\left(\frac{x}{2}\right)J_\mu^{Z_0}\left(-\frac{x}{2}\right)\right)|P_1\rangle &= \langle P_2|\overline{\psi}_u\left(\frac{x}{2}\right)g_u\gamma_\nu S(x)\gamma_\mu(g_{uV}^Z + g_{uA}^Z\gamma^5)\psi_u\left(-\frac{x}{2}\right) - \\ &\quad - \overline{\psi}_d\left(\frac{x}{2}\right)g_d\gamma_\nu S(x)\gamma_\mu(g_{dV}^Z + g_{dA}^Z\gamma^5)\psi_d\left(-\frac{x}{2}\right) + \\ &\quad + \overline{\psi}_u\left(\frac{x}{2}\right)\gamma_\mu(g_{uV}^Z + g_{uA}^Z\gamma^5)S(-x)g_u\gamma_\nu\psi_u\left(\frac{x}{2}\right) - \\ &\quad - \overline{\psi}_d\left(\frac{x}{2}\right)\gamma_\mu(g_{dV}^Z + g_{dA}^Z\gamma^5)S(-x)g_d\gamma_\nu\psi_d\left(\frac{x}{2}\right)|P_1\rangle\,. \end{aligned} \quad (4.3)$$

The coefficients used in eqs. (4.2), (4.3) g_V^Z and g_A^Z, are

$$\begin{aligned} g_{uV}^Z &= \frac{1}{2} + \frac{4}{3}\sin^2\theta_W \qquad g_{uA}^Z = -\frac{1}{2} \\ g_{dV}^Z &= -\frac{1}{2} + \frac{2}{3}\sin^2\theta_W \qquad g_{dA}^Z = \frac{1}{2}\,, \end{aligned} \quad (4.4)$$

and

$$g_u = \frac{2}{3}\,, \qquad g_d = \frac{1}{3} \tag{4.5}$$

are the absolute values of the charges of the up and down quarks in units of the electron charge.

The function $S(x)$ denotes the free quark propagator

$$S(x) \approx \frac{i\not{x}}{2\pi^2(x^2 - i\epsilon)^2}\,. \tag{4.6}$$

After some standard identities for the γ's products

$$\begin{aligned}
\gamma_\mu\gamma_\alpha\gamma_\nu &= S_{\mu\alpha\nu\beta}\gamma^\beta + i\epsilon_{\mu\alpha\nu\beta}\gamma^5\gamma^\beta\,,\\
\gamma_\mu\gamma_\alpha\gamma_\nu\gamma^5 &= S_{\mu\alpha\nu\beta}\gamma^\beta\gamma^5 - i\epsilon_{\mu\alpha\nu\beta}\gamma^\beta\,,\\
S_{\mu\alpha\nu\beta} &= (g_{\mu\alpha}g_{\nu\beta} + g_{\nu\alpha}g_{\mu\beta} - g_{\mu\nu}g_{\alpha\beta})\,,
\end{aligned} \tag{4.7}$$

we rewrite the correlators as

$$\begin{aligned}
&T_{\mu\nu} = i\int d^4x \frac{e^{iqx}x^\alpha}{2\pi^2(x^2 - i\epsilon)^2} \times\\
&\times\langle P_2|\Big[g_u g_{uV}\Big(S_{\mu\alpha\nu\beta}O_u^\beta - i\epsilon_{\mu\alpha\nu\beta}O_u^{5\beta}\Big) - g_u g_{uA}\Big(S_{\mu\alpha\nu\beta}\tilde{O}_u^{5\beta} - i\epsilon_{\mu\alpha\nu\beta}\tilde{O}_u^\beta\Big) -\\
&\quad - g_d g_{dV}\Big(S_{\mu\alpha\nu\beta}O_d^\beta - i\epsilon_{\mu\alpha\nu\beta}O_d^{5\beta}\Big) + g_d g_{dA}\Big(S_{\mu\alpha\nu\beta}\tilde{O}_d^{5\beta} - i\epsilon_{\mu\alpha\nu\beta}\tilde{O}_d^\beta\Big)\Big]|P_1\rangle\,.
\end{aligned} \tag{4.8}$$

The x-dependence of the operators in the former equations was suppressed.

Whence the relevant operators are denoted by

$$\begin{aligned}
\tilde{O}_a^\beta\Big(\frac{x}{2},-\frac{x}{2}\Big) &= \overline{\psi}_a\Big(\frac{x}{2}\Big)\gamma^\beta\psi_a\Big(-\frac{x}{2}\Big) + \overline{\psi}_a(-\frac{x}{2}\Big)\gamma^\beta\psi_a\Big(\frac{x}{2}\Big),\\
\tilde{O}_a^{5\beta}\Big(\frac{x}{2},-\frac{x}{2}\Big) &= \overline{\psi}_a\Big(\frac{x}{2}\Big)\gamma^5\gamma^\beta\psi_a\Big(-\frac{x}{2}\Big) - \overline{\psi}_a\Big(-\frac{x}{2}\Big)\gamma^5\gamma^\beta\psi_a\Big(\frac{x}{2}\Big),\\
O_a^\beta\Big(\frac{x}{2},-\frac{x}{2}\Big) &= \overline{\psi}_a\Big(\frac{x}{2}\Big)\gamma^\beta\psi_a\Big(-\frac{x}{2}\Big) - \overline{\psi}_a\Big(-\frac{x}{2}\Big)\gamma^\beta\psi_a\Big(\frac{x}{2}\Big),\\
O_a^{5\beta}\Big(\frac{x}{2},-\frac{x}{2}\Big) &= \overline{\psi}_a\Big(\frac{x}{2}\Big)\gamma^5\gamma^\beta\psi_a\Big(-\frac{x}{2}\Big) + \overline{\psi}_a\Big(-\frac{x}{2}\Big)\gamma^5\gamma^\beta\psi_a\Big(\frac{x}{2}\Big)\,,
\end{aligned} \tag{4.9}$$

where a is a flavour index.

5. Phases of the amplitude

The numerical computation of the cross section requires a prescription for a correct handling of the singularities in the integration region at $z = \pm\xi$. The best way to proceed is to work out explicitly the structure of the factorization formula of the amplitude using the Feynman prescription for going around the singularities, thereby isolating a principal value integral (P.V., which is real) and an imaginary contribution coming from the δ function term. A P.V. integral is expressed in terms of "plus" distributions and of logarithmic terms, as illustrated below. The expression of the factorization formula of the process in the parton model, in which $\alpha(z)$ and $\beta(z)$ appear as factors in the coefficient functions, is then given by

$$
\begin{aligned}
\mathcal{M}_{fi} =\; & J^{\mu}_{Z}(q_1)D(q_1)\epsilon^{\nu *}(q_1-\Delta)\times \\
& \times\Bigg\{\frac{i}{2}\tilde{g}g_u U_v\int_{-1}^{1}dz(\tilde{n}^{\mu}n^{\nu}+\tilde{n}^{\nu}n^{\mu}-g^{\mu\nu})\times \\
& \quad\times\alpha(z)\Bigg[H^{u}(z,\xi,\Delta^2)\overline{U}(P_2)\not{n}\;U(P_1)+E^{u}(z,\xi,\Delta^2)\overline{U}(P_2)\frac{i\sigma^{\mu\nu}n_{\mu}\Delta_{\nu}}{2M}U(P_1)\Bigg]+ \\
& \quad+\beta(z)i\epsilon^{\mu\nu\alpha\beta}\tilde{n}_{\alpha}n_{\beta}\Bigg[\tilde{H}^{u}(z,\xi,\Delta^2)\overline{U}(P_2)\not{n}\;\gamma^5U(P_1)+ \\
& \qquad\qquad+\tilde{E}^{u}(z,\xi,\Delta^2)\overline{U}(P_2)\gamma^5(\Delta\cdot n)U(P_1)\Bigg]+ \\
& \quad+\frac{i}{2}\tilde{g}g_dD_v\int_{-1}^{1}dz\{u\to d\}-\frac{i}{2}\tilde{g}g_u\int_{-1}^{1}dz(-\tilde{n}^{\mu}n^{\nu}-\tilde{n}^{\nu}n^{\mu}+g^{\mu\nu})\times \\
& \quad\times\alpha(z)\Bigg[\tilde{H}^{u}(z,\xi,\Delta^2)\overline{U}(P_2)\not{n}\;\gamma^5U(P_1)+\tilde{E}^{u}(z,\xi,\Delta^2)\overline{U}(P_2)\frac{i\gamma^5\Delta\cdot n}{2M}U(P_1)\Bigg]+ \\
& \quad+\beta(z)i\epsilon^{\mu\nu\alpha\beta}\tilde{n}_{\alpha}n_{\beta}\Bigg[H^{u}(z,\xi,\Delta^2)\overline{U}(P_2)\not{n}\;U(P_1)+ \\
& \qquad\qquad+E^{u}(z,\xi,\Delta^2)\overline{U}(P_2)\frac{i\sigma^{\mu\nu}n_{\mu}\Delta_{\nu}}{2M}(P_1)\Bigg]- \\
& \quad-\frac{i}{2}\tilde{g}g_d\int_{-1}^{1}dz\{u\to d\}\Bigg\}.
\end{aligned}
\tag{5.1}
$$

To handle the singularity on the path of integration in the factorization formula, as we have already mentioned, we use the Feynman ($i\epsilon$) prescription, thereby generating imaginary parts. In particular, any standard integral containing imaginary parts is then separated into real and imaginary contributions as

$$
\int dz\frac{T(z)}{z\mp\xi\pm i\epsilon}=PV\int_{-1}^{1}dz\frac{T(z)}{z\mp\xi}\;\mp i\pi T(\pm\xi)
\tag{5.2}
$$

for a real coefficient $T(z)$. We then rewrite the P.V. integral in terms of "plus" distributions

$$
\begin{aligned}
P.V.\int_{-1}^{1}dz\frac{H(z)}{z-\xi} &= \int_{-1}^{1}dz\frac{H(z)-H(\xi)}{z-\xi}+H(\xi)\log\left(\frac{1-\xi}{1+\xi}\right) \\
&= \int_{-1}^{1}dz\mathcal{Q}(z)H(z)+\int_{-1}^{1}dz\bar{\mathcal{Q}}(z)H(z)+H(\xi)\log\left(\frac{1-\xi}{1+\xi}\right)
\end{aligned}
\tag{5.3}
$$

where

$$
\begin{aligned}
\mathcal{Q}(z) &= \theta(-1\leq z\leq\xi)\frac{1}{(z-\xi)_{+}} \\
&= \theta(-1\leq z\leq\xi)\left(\frac{\theta(z<\xi)}{(z-\xi)}-\delta(z-\xi)\int_{-1}^{\xi}\frac{dz}{(z-\xi)}\right)
\end{aligned}
$$

JHEP02(2005)038

$$
\begin{aligned}
\bar{\mathcal{Q}}(z) &= \theta(\xi \le z \le 1)\frac{1}{(z-\xi)_+} \\
&= \theta(-1 \le z \le \xi)\left(\frac{\theta(z>\xi)}{(z-\xi)} - \delta(z-\xi)\int_\xi^1 \frac{dz}{(z-\xi)}\right)
\end{aligned} \tag{5.4}
$$

and the integrals are discretized using finite elements methods, in order to have high numerical accuracy. This last point is illustrated in appendix C, where the computations are done analytically on a grid and then the grid spacing is sent to zero.

We can now proceed and compute the cross section. We define the scalar amplitude

$$
\mathcal{M}_{fi} = J^\mu_{\rm Lep}(q_1)D(q_1)T^{\mu\nu}\epsilon^{*\nu}(q_1-\Delta) \tag{5.5}
$$

where $D(q_1)$ is the Z_0 propagator in the Feynman gauge and $J^\mu_{\rm Lep}(q_1)$ is the leptonic current and we have introduced the polarization vector for the final state photon ϵ^ν.

In particular, for the squared amplitude we have

$$
|\mathcal{M}_{fi}|^2 = -L^{\mu\lambda}D(q_1)^2 T_{\mu\nu}T^{*\nu}_\lambda \tag{5.6}
$$

which is given, more specifically, by

$$
|\mathcal{M}|^2 = \int_{-1}^1 dz \int_{-1}^1 dz' \left(K_1(z,z')\alpha(z)\alpha^*(z') + K_2(z,z')\beta(z)\beta^*(z')\right) \tag{5.7}
$$

with K_1 and K_2 real functions, combinations of the generalized distributions $(H, \tilde{H}, E, \tilde{E})$ with appropriate kinematical factors. Mixed contributions proportional to $\alpha(z)\beta^*(z')$ and $\beta(z)\alpha^*(z')$ cancel both in their real and imaginary parts and as such do not contribute to the phases. A similar result holds also for the pure electromagnetic case.

After some further manipulations, we finally rewrite the squared amplitude in terms of a P.V. contribution plus some additional terms coming from the imaginary parts

$$
\begin{aligned}
|\mathcal{M}|^2 &= P.V. \int_{-1}^1 dz \int_{-1}^1 dz' \left(K_1(z,z')\alpha(z)\alpha^*(z') + K_2(z,z')\beta(z)\beta^*(z')\right) + \\
&+\pi^2 \left(K_1(\xi,\xi) - K_1(\xi,-\xi) - K_1((-\xi,\xi) + K_1(-\xi,-\xi)\right) + \\
&+\pi^2 \left(K_2(\xi,\xi) + K_2(\xi,-\xi) + K_2((-\xi,\xi) + K_2(-\xi,-\xi)\right)
\end{aligned} \tag{5.8}
$$

which will be analized numerically in the sections below. In order to proceed with the numerical result, it is necessary to review the standard construction of the nonforward parton distribution functions in terms of the forward distributions, which is the topic of the next section.

6. Construction of the input distributions

The computation of the cross section proceeds rather straightforwardly, though the construction of the initial conditions is more involved compared to the forward (DIS) case. This construction has been worked out in several papers [15, 16, 17, 18, 19, 8] in the case of standard DVCS, using a diagonal input appropriately extended to the non-diagonal kinematics. Different types of nonforward parton distribution, all widely used in the numerical implementations have been put forward, beside Ji's original distributions, which we will be using in order to construct the initial conditions for our process.

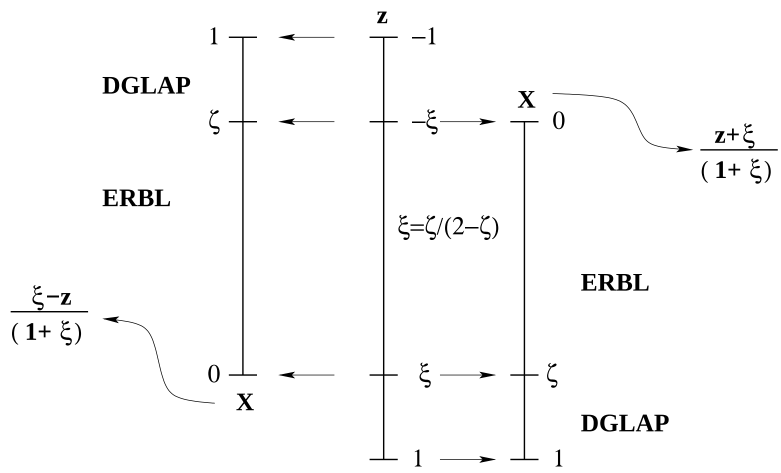

Figure 4: The relationship between $\mathcal{F}^q(X,\zeta)$, $\mathcal{F}^{\bar{q}}(X,\zeta)$ and Ji's function $H^q(z,\xi)$.

For our purposes it will be useful to introduce Golec-Biernat and Martin's (GBM) distributions [17] at an intermediate step, which are linearly related to Ji's distributions.

We recall, at this point, that the quark distributions $H_q(z,\xi)$ have support in $z \in [-1,1]$, describing both quark and antiquark distributions for $z>0$ and $z<0$ respectively. In terms of GBM distributions, two distinct distributions $\hat{\mathcal{F}}^{\bar{q}}(X,\zeta)$ and $\hat{\mathcal{F}}^q(X,\zeta)$ with $0 \leq X \leq 1$ are needed in order to cover the same information contained in Ji's distributions using only a positive scaling variable (X). In the region $X \in (\zeta, 1]$ the functions $\hat{\mathcal{F}}^q$ and $\hat{\mathcal{F}}^{\bar{q}}$ are independent, but if $X \leq \zeta$ they are related to each other, as shown in the (by now standard) plot in figure 4.

In this new variable (X) the DGLAP region is described by $X > \zeta$ ($|z| > \xi$), and the ERBL region by $X < \zeta$ ($|z| < \xi$). In the ERBL region, $\hat{\mathcal{F}}^q$ and $\hat{\mathcal{F}}^{\bar{q}}$ are not independent.

The relation between $H(z,\xi)$ and $\hat{\mathcal{F}}^q(X,\zeta)$ can be obtained explicitly [20] as follows: for $z \in [-\xi, 1]$ we have

$$\hat{\mathcal{F}}^{q,i}\left(X = \frac{z+\xi}{1+\xi}, \zeta\right) = \frac{H^{q,i}(z,\xi)}{1-\zeta/2}\,, \tag{6.1}$$

and for $z \in [-1, \xi]$

$$\hat{\mathcal{F}}^{\bar{q},i}\left(X = \frac{\xi - z}{1+\xi}, \zeta\right) = -\frac{H^{q,i}(z,\xi)}{1-\zeta/2}\,, \tag{6.2}$$

where i is a flavour index.

In our calculations we use a simplified model for the GPD's where the Δ^2 dependence can be factorized as follows [21, 15]

$$\begin{aligned} H^i(z,\xi,\Delta^2,Q^2) &= F_1^i\,(\Delta^2) q^i(z,\xi,Q^2) \\ \tilde{H}^i(z,\xi,\Delta^2,Q^2) &= G_1^i(\Delta^2)\,\Delta q^i(z,\xi,Q^2) \\ E^i(z,\xi,\Delta^2,Q^2) &= F_2^i(\Delta^2)\, r^i(z,\xi,Q^2) \end{aligned} \tag{6.3}$$

where $q^i(z)$ and $\Delta q^i(z)$ are obtained from the standard non-polarized and longitudinally polarized (forward) quark distributions using a specific diagonal ansatz [22].

The ansatz $r^i(z,\xi) = q^i(z,\xi)$ is also necessary in order for the quark sum rule to hold [23]. Analogously, in the case of the $\tilde{E}^i$ distributions [8, 24, 25] one can use the special model

$$\tilde{E}^u = \tilde{E}^d = \frac{1}{2\xi}\theta(\xi-|z|)\phi_\pi\left(\frac{z}{\xi}\right)g_\pi(\Delta^2)\,, \quad g_\pi(\Delta^2) = \frac{4g_A^{(3)}M^2}{m_\pi^2-\Delta^2}\,, \quad \phi_\pi(x) = \frac{4}{3}(1-x^2) \tag{6.4}$$

valid at small Δ^2, where $g_A^{(3)} = 1.267$, M is the nucleon mass and m_π is the pion mass, with the normalization

$$F_1^i(0) = G_1^i(0) = 1\,. \tag{6.5}$$

Notice that, analogously to the H distributions, $q^i(z,\xi,Q^2)$ and $\Delta q^i(z,\xi,Q^2)$, which describe the $\Delta^2 = 0$ limit of the H-distributions, have support in $[-1,1]$ and, again, they describe quark distributions (for $z > 0$) and antiquark distributions (for $z < 0$)

$$\begin{aligned}\bar{q}^i(z,\xi,Q^2) &= -q^i(-z,\xi,Q^2)\\ \Delta\bar{q}^i(z,\xi,Q^2) &= \Delta q^i(-z,\xi,Q^2)\,.\end{aligned} \tag{6.6}$$

Now we're going to estabilish a connection between the $q(z,\xi,\bar{Q}^2)$ and the $\hat{\mathcal{F}}^q(X,\zeta)$ functions, which is done using Radyushkin's nonforward "double distributions" [8]. The construction of the input distributions, in correspondence of an input scale Q_0, is performed following a standard strategy. This consists in generating nonforward double distributions $f(x,y)$ from the forward ones $(f(x))$ using a "profile function" $\pi(x,y)$ [7]

$$f(y,x) = \pi(y,x)f(x)\,, \tag{6.7}$$

where we just recall that the $\pi(y,x)$ function can be represented by

$$\pi(y,x) = \frac{3}{4}\frac{[1-|x|]^2-y^2}{[1-|x|]^3}\,, \tag{6.8}$$

taken to be of an asymptotic shape (see ref. [7, 16]) for quarks and gluons. A more general profile is given by

$$\pi(x,y) = \frac{\Gamma(2b+2)}{2^{2b+1}\Gamma^2(b+1)}\frac{[(1-|x|)^2-y^2]^b}{(1-|x|)^{2b+1}} \tag{6.9}$$

and normalized so that

$$\int_{-1+|x|}^{1-|x|} dy\, \pi(x,y) = 1\,. \tag{6.10}$$

b parameterizes the size of the skewing effects starting from the diagonal input. Other choices of the profile function are also possible. For instance, the double distributions (DD) defined above have to satisfy a symmetry constraint based on hermiticity. This demands that these must be symmetric with respect to the exchange $y \longleftrightarrow 1-x-y$, and a profile function which respects this symmetry constraint is given by [26]

$$\pi(x,y) = \frac{6y(1-x-y)}{(1-x)^3}\,. \tag{6.11}$$

This symmetry is crucial for establishing proper analytical properties of meson production amplitudes. We will be using below this profile and compare the cross section obtained with it against the one obtained with (6.9).

Now we are able to generate distributions $q(z, \xi, Q^2)$ in the z variable at $\Delta^2 = 0$, $q(z, \xi, Q^2)$, by integrating over the longitudinal fraction of momentum exchange y characteristic of the double distributions

$$q(z, \xi, Q^2) = \int_{-1}^{1} dx' \int_{-1+|x'|}^{1-|x'|} dy' \delta(x' + \xi y' - z) f(y', x', Q^2) \,. \tag{6.12}$$

Using (6.12) and the expression of the profile functions introduced above, the GBM distributions are generated by the relation

$$\hat{\mathcal{F}}^{q,a}(X, \zeta) = \frac{2}{\zeta} \int_{\frac{X-\zeta}{1-\zeta}}^{X} dx' \pi^q \left(x', \frac{2}{\zeta}(X - x') + x' - 1 \right) q^a(x') \,. \tag{6.13}$$

with a similar expression for the anti-quark distributions in the DGLAP region $X > \zeta$ ($z < -\xi$)

$$\hat{\mathcal{F}}^{\bar{q},a}(X, \zeta) = \frac{2}{\zeta} \int_{-X}^{\frac{-X+\zeta}{1-\zeta}} dx' \pi^q \left(x', -\frac{2}{\zeta}(X + x') + x' + 1 \right) \bar{q}^a(|x'|) \,. \tag{6.14}$$

In the ERBL region, $X < \zeta$ ($|z| < \xi$), after the integration over y, we are left with the sum of two integrals

$$\begin{aligned}
\hat{\mathcal{F}}^{q,a}(X, \zeta) &= \frac{2}{\zeta} \Bigg[\int_0^X dx' \pi^q \left(x', \frac{2}{\zeta}(X - x') + x' - 1 \right) q^a(x') - \\
&\quad - \int_{X-\zeta}^{0} dx' \pi^q \left(x', \frac{2}{\zeta}(X - x') + x' - 1 \right) \bar{q}^a(|x'|) \Bigg] , \\
\hat{\mathcal{F}}^{\bar{q},a}(X, \zeta) &= -\frac{2}{\zeta} \Bigg[\int_0^{\zeta - X} dx' \pi^q \left(x', -\frac{2}{\zeta}(X + x') + x' + 1 \right) q^a(x') - \\
&\quad - \int_{-X}^{0} dx' \pi^q \left(x', -\frac{2}{\zeta}(X + x') + x' + 1 \right) \bar{q}^a(|x'|) \Bigg] .
\end{aligned} \tag{6.15}$$

Solving numerically the integrals we obtain the value of the function $\mathcal{F}^q$s on a grid, and using eqs. (6.1) and 6.2 we end up with the numerical form of the H-distributions. We have used diagonal parton distribution functions at $0.26\,\mathrm{GeV}^2$ [22] and the results of our numerical implementation can be visualized in figures 5 and 6.

7. The differential cross section

Our kinematical setup is illustrated in figure 8, and we choose momenta in the target frame with the following parameterizations

$$\begin{aligned}
l &= (E, 0, 0, E) \,, \quad l' = \left(E', E' \cos\phi_\nu \sin\theta_\nu, E' \sin\phi_\nu \sin\theta_\nu, E' \cos\theta_\nu \right) , \\
P_1 &= (M, 0, 0, 0) \,, \quad P_2 = (E_2, |P_2| \cos\phi_N \sin\theta_N, |P_2| \sin\phi_N \sin\theta_N, |P_2| \cos\theta_N)
\end{aligned} \tag{7.1}$$

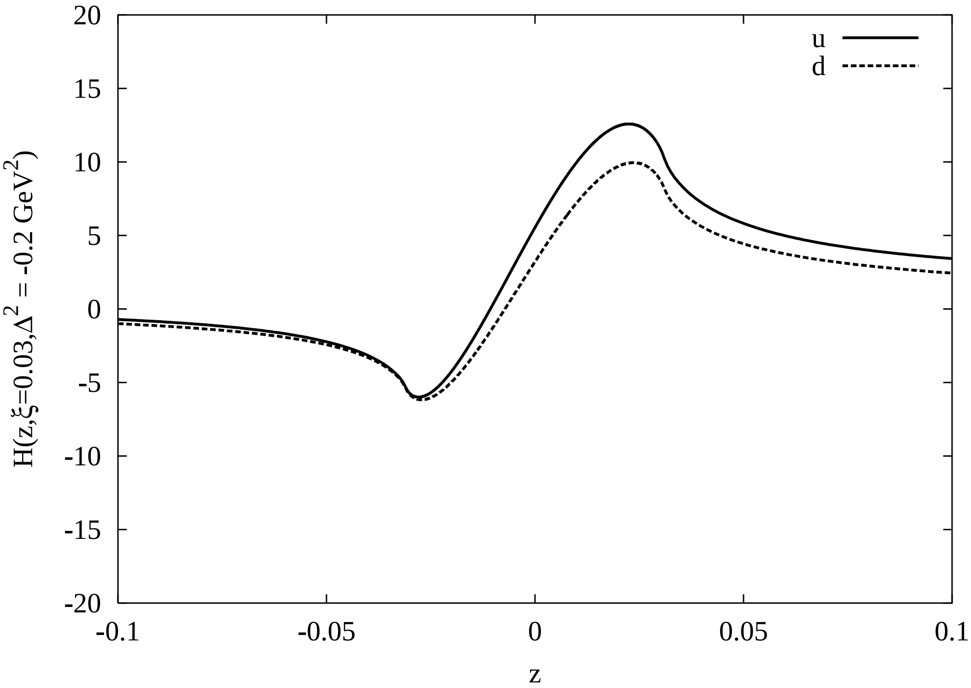

Figure 5: GPD's H_u and H_d generated by the diagonal parton distribution with a profile function (6.9) at an initial $0.26\,\mathrm{GeV}^2$.

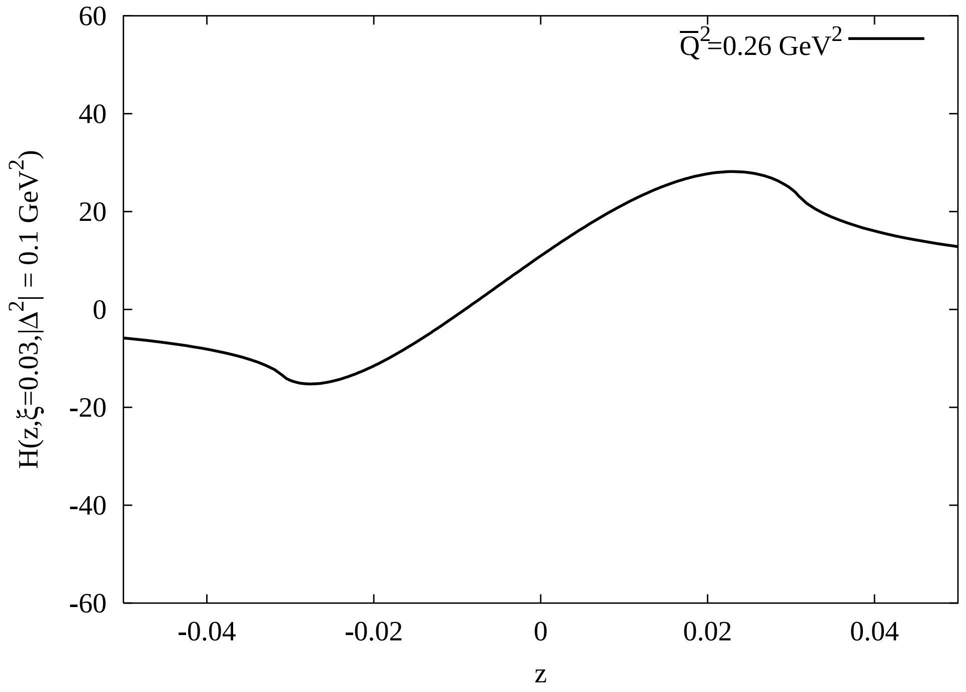

Figure 6: GPD's flavour singlet combination at $0.26\,\mathrm{GeV}^2$ generated with a profile (6.9).

where the incoming neutrino is taken in the positive $\hat{z}$-direction and the nucleon is originally at rest. The first plane is identified by the momenta of the final state nucleon and of the

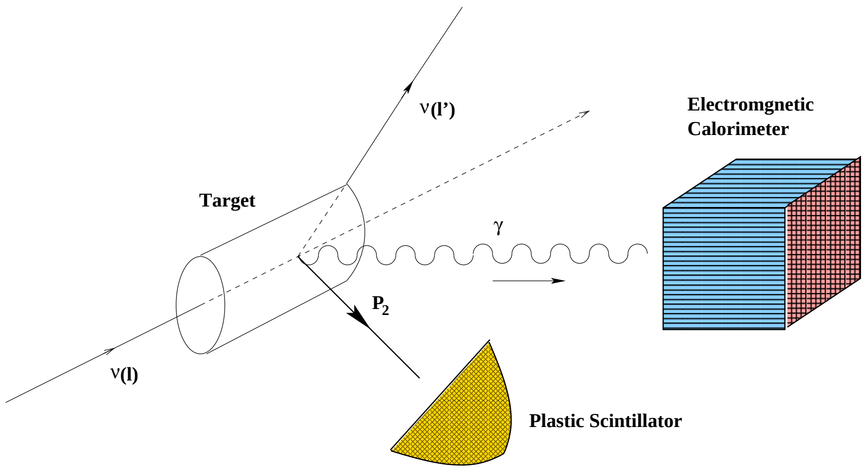

Figure 7: A pictorial description of the DVNS experimental setup, where the recoiled nucleon is detected in coincidence with a final state photon.

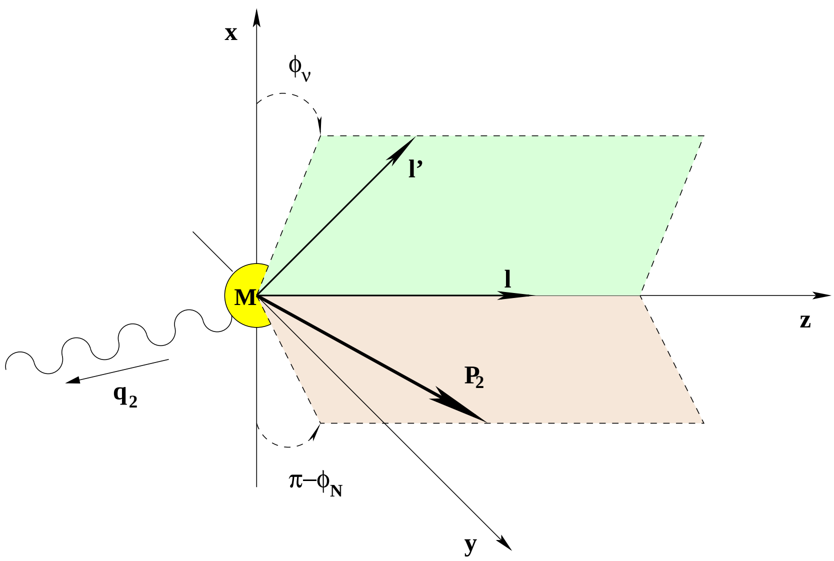

Figure 8: Kinematics of the process $\nu(l)N(P_1) \to \nu(l')N(P_2)\gamma(q_2)$.

incoming neutrino, while the second plane is spanned by the final state neutrino and the same $\hat{z}$-axis. ϕ_ν is the angle between the $\hat{x}$ direction and the second plane, while ϕ_N is taken between the plane of the scattered nucleon and the same $\hat{x}$ axis. We recall that the general form of a differential cross section is given by

$$d\sigma = \frac{1}{4(l \cdot P_1)} |\mathcal{M}_{fi}|^2 (2\pi)^4 \delta^{(4)}(l + P_1 - P_2 - l' - q_2) \frac{d^3\vec{l'}}{2l'^0(2\pi)^3} \frac{d^3\vec{P_2}}{2P_2^0(2\pi)^3} \frac{d^3\vec{q_2}}{2q_2^0(2\pi)^3} \tag{7.2}$$

and it will be useful to express it in terms of standard quantities appearing in a standard DIS process such as Bjorken variable x, inelasticity parameter y, the momentum transfer plus some additional kinematical variables typical of DVCS such as the asymmetry parameter ξ and Δ^2.

We will be using the relations

$$
\begin{aligned}
\bar{q}^2 &= -\frac{1}{2}q_1^2\left(1-\frac{\Delta^2}{2q_1^2}\right) \approx \frac{1}{2}Q^2 \\
\xi &= \frac{x\left(1-\frac{\Delta^2}{2q_1^2}\right)}{2-x\left(1-\frac{\Delta^2}{2q_1^2}\right)} \approx \frac{2x}{2-x}
\end{aligned}
\tag{7.3}
$$

in the final computation of the cross section. It is also important to note that Δ^2 has to satisfy a kinematical constraint

$$
\Delta^2_{\rm min} = -\frac{M^2x^2}{1-x+\frac{xM^2}{Q^2}}\left(1+\mathcal{O}\left(\frac{M^2}{Q^2}\right)\right). \tag{7.4}
$$

One possible cross section to study, in analogy to the DVCS case [27], is the following

$$
\frac{d\sigma}{dxdQ^2d|\Delta^2|d\phi_r} = \frac{y}{Q^2}\frac{d\sigma}{dxdyd|\Delta^2|d\phi_r} = \frac{xy^2}{8\pi Q^4}\left(1+\frac{4M^2x^2}{Q^2}\right)^{-\frac{1}{2}}|\mathcal{M}_{fi}|^2\,, \tag{7.5}
$$

where ϕ_r is the angle between the lepton and the hadron scattering planes. To proceed we also need the relations

$$
\begin{aligned}
l\cdot n &= \left[\frac{Q^2}{2xy}-\frac{(1+\xi)}{2\xi}\frac{Q^2}{2}\right]\chi\,, \\
l\cdot\tilde{n} &= \frac{Q^2}{2\xi}+\frac{Q^2}{4\xi^2}\left[\frac{Q^2}{2xy}-\frac{(1+\xi)}{2\xi}\frac{Q^2}{2}\right]\chi\,, \\
n\cdot q_1 &= \frac{2x}{x-2}\,, \qquad \tilde{n}\cdot q_1 = Q^2\frac{(2-x)}{8x}\,,
\end{aligned}
\tag{7.6}
$$

where χ is given by

$$
\chi = \frac{\xi}{\frac{1+\xi}{2}\frac{Q^2}{4\xi}+\frac{\xi(1-\xi)}{2}\frac{\overline{M}^2}{2}}\,. \tag{7.7}
$$

After some manipulations we obtain a simplified expression for $|\mathcal{M}_{fi}|^2$, similarly to eq. (5.7)

$$
\begin{aligned}
|\mathcal{M}_{fi}|^2 = &\int_{-1}^{1}dz\int_{-1}^{1}dz'\left[A_1(z,z',x,t,Q^2)\alpha(z)\alpha^*(z')+A_2(z,z',x,t,Q^2)\beta(z)\beta^*(z')\right]\times \\
&\times\Big[-2Q^2\left(4M^2-t\right)(x-2)^2\,(x-1)\,x^2y+(t-4M^2)^2(x-1)^2\,x^4y^2+ \\
&\quad +Q^4(x-2)^4\left(2-2y+y^2\right)\Big] \\
&\times\left[2M^2({M_Z}^2+Q^2)^2\,(x-2)^2\left[Q^2(x-2)^2-(4M^2-t)(-1+x)x^2\right]^2y^2\right]^{-1}
\end{aligned}
\tag{7.8}
$$

where $A_1(z,z',x,t,Q^2)$ and $A_2(z,z',x,t,Q^2)$ are functions of the invariants of the process and of the entire set of GPD's. Their explicit form is given in appendix D. As we have already mentioned, the (z,z') integration is be done by using the Feynman prescription to extract the phases and then using the distributional identities (5.3) and (5.4). For numerical accuracy we have discretized the final integrals by finite element methods, as shown in appendix C.

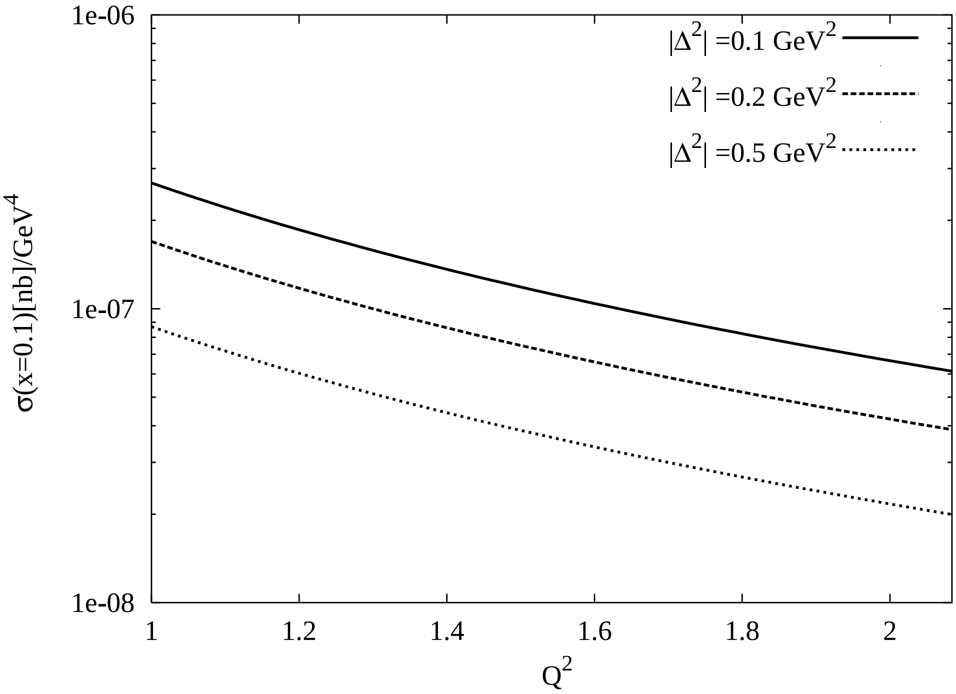

Figure 9: DVCS cross section at $x = 0.1$ and center of mass energy $ME = 10\,\mathrm{GeV}^2$ using the profile (6.9).

We have plotted the differential cross section as a function of Q^2, for various values of Δ^2 and at fixed x values. We have used both the profile given by (6.9) (figures 9–12) and the one given in eq. (6.11) (figures 13 and 14) and their direct comparison in a specific kinematical region (figure 15). The different profiles generate differences in the cross sections especially for larger Δ^2 values. Notice also that the DVNS cross section decreases rather sharply with Δ^2, at the same time it increases appreciably with x. The results shown are comparable with other cross sections evaluated in the quasi-elastic region ($\approx 10^{-5}$ nb) for charged and neutral current interactions, and appear to be sizeable. Coherence effects due to neutral current interactions with heavy nuclei, in particular with the neutron component may substantially increase the size of the cross sections, with an enhancement proportional to N^2, where N is the number of neutrons [28], though an accurate quantification of these effects requires a special study [29] which is underway. It is worth to emphasize that in the past this contribution had never been included in the study of neutrino-nucleon interactions since very little was known about the intermediate energy kinematics in QCD from the point of view of factorization. It seems obvious to us that with the new developments now taking place in the study of QCD at intermediate energy, especially in the case of the generalized Bjorken region, of which the deeply virtual scattering limit is just a special case, it will be of wide interest to quantify with accuracy the role of these new contributions for neutrino factories. In general, one expects that electromagnetic effects are suppressed compared to the standard (hadronic) deeply inelastic cross section, and this has led in the past to a parameterization of the intermediate energy cross section as either dominated by the quasi elastic region and/or by the DIS region at higher energies, as we have mentioned in our

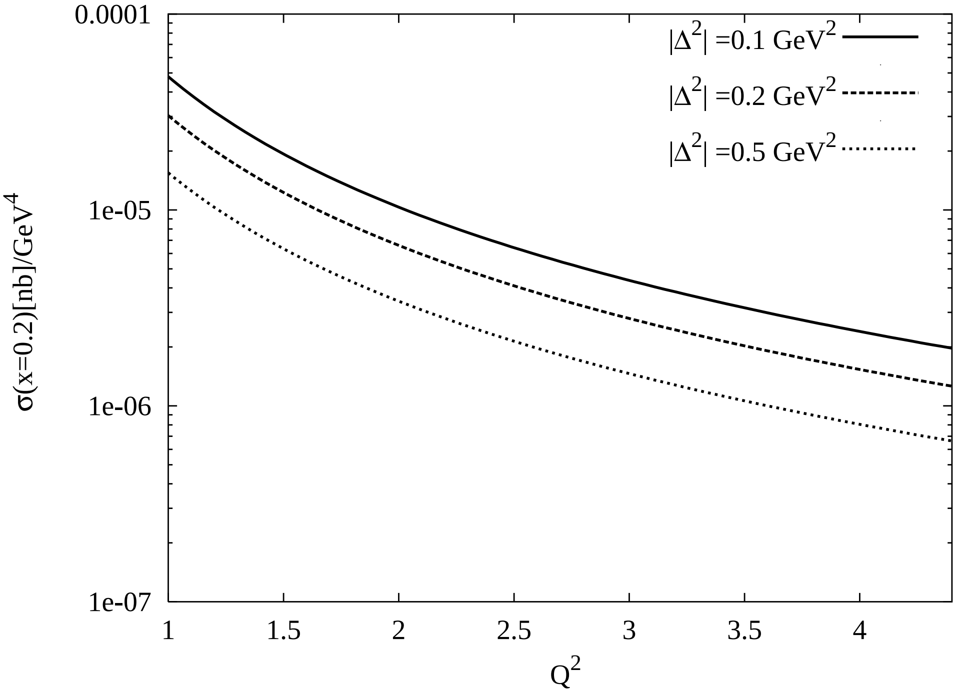

Figure 10: DVCS cross section at $x = 0.2$ and center of mass energy $ME = 10\,\mathrm{GeV}^2$ using the profile (6.9).

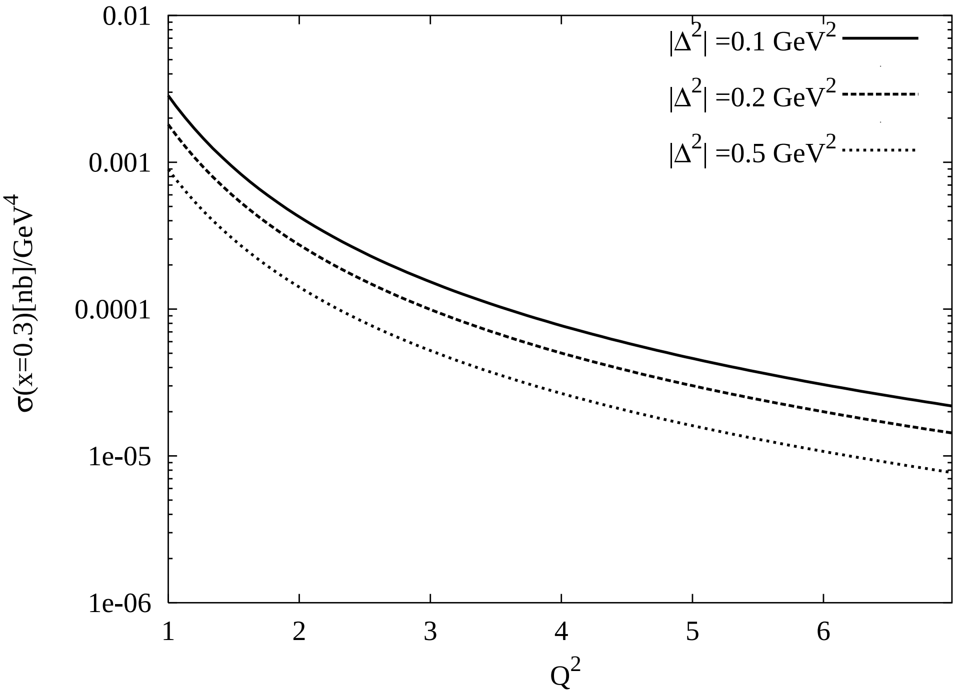

Figure 11: DVCS cross section at $x = 0.3$ and center of mass energy $ME = 10\,\mathrm{GeV}^2$ using the profile (6.9).

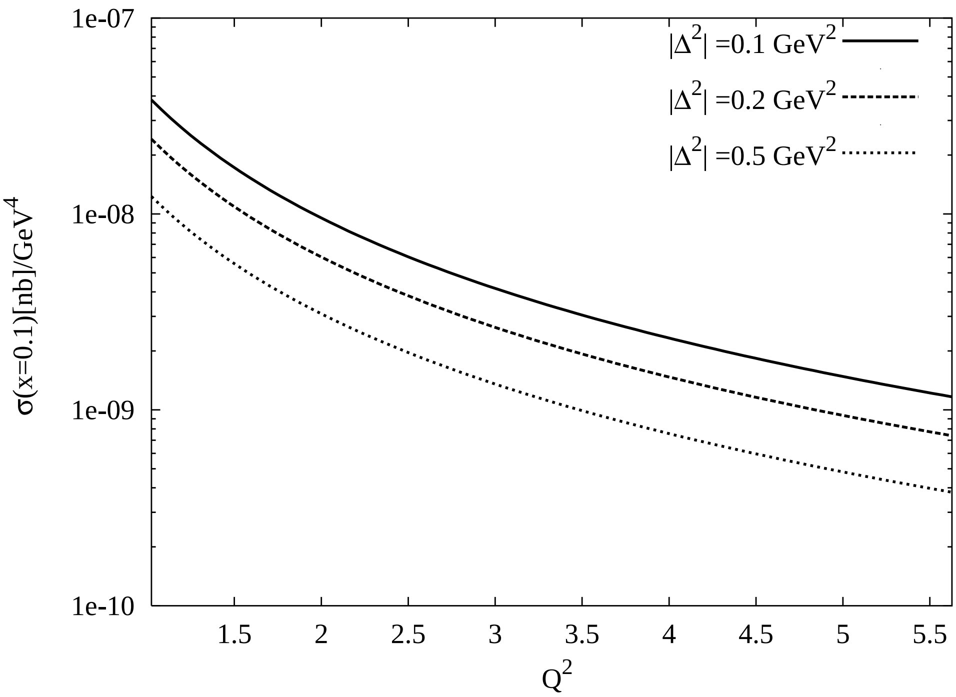

Figure 12: DVCS cross section at $x = 0.1$ and center of mass energy $ME = 27\,\mathrm{GeV}^2$ using the profile (6.9).

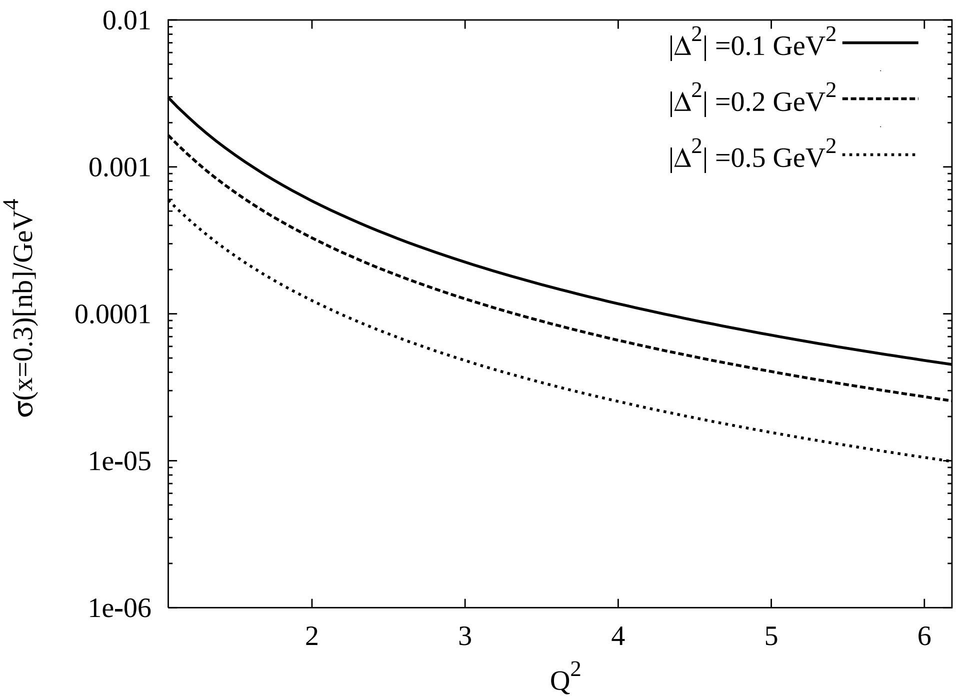

Figure 13: DVCS cross section at $x = 0.3$ and center of mass energy $ME = 10\,\mathrm{GeV}^2$ with non-forward partons distribution functions generated by the profile function (6.11).

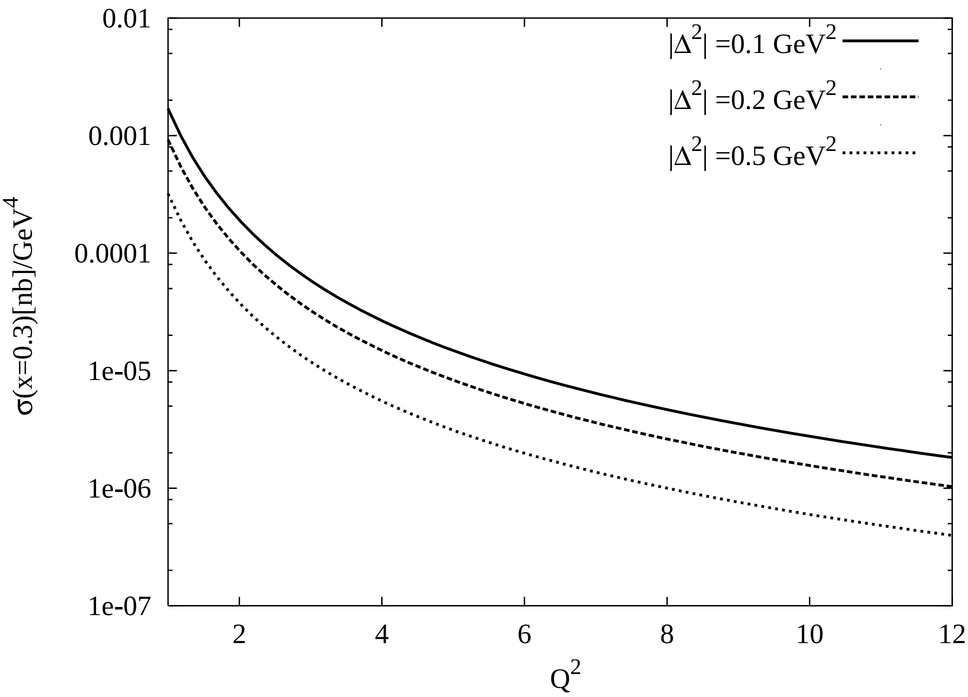

Figure 14: DVCS cross section at $x = 0.3$ and center of mass energy $ME = 27\,\mathrm{GeV}^2$ with non-forward partons distribution functions generated by the profile function (6.11).

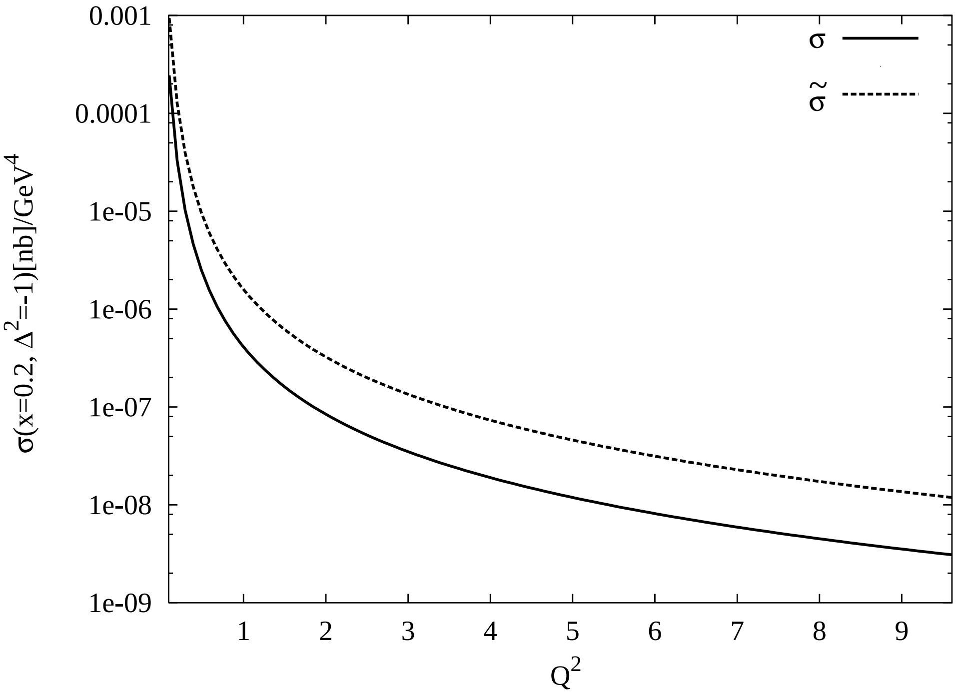

Figure 15: DVCS cross sections at $x = 0.2$ and center of mass energy $ME = 27\,\mathrm{GeV}^2$, $\tilde{\sigma}$ is obtained using profile (6.11).

introduction. However, the exclusive cross section has some special positive features, one of them being to provide a clean signal for the detection of weakly interacting particles, and we expect that this aspect is going to be of relevance at experimental level.

8. Conclusions

We have presented an extension of the standard DVCS process to the case of one neutral current exchange, describing the scattering of a neutrino off a proton in the parton model. We have described the leading twist behaviour of the cross section; we have found that this is comparable to other typical neutrino cross sections and discussed its forward or DIS limit. We have presented a complete formalism for the study of these processes in the parton model. The process is the natural generalization of DIS with neutral currents and relies on the notion of Generalized Parton Distributions, new constructs in the parton model which have received considerable attention in recent years. The possible applications of these new processes are manifold and we hope to return in the near future with a discussion of some of the issues not addressed in this work.

Acknowledgments

We warmly thank J.D. Vergados for illuminating discussions on the detectability of this process, and Giovanni Chirilli of Old Dominion University for discussions and for collaborating on the derivation of the results of section 5. The work of C.C. is supported in part under the grant HPRN-CT-2000-00121. C.C. and M.G. thank T.N. Tomaras and E. Kiritsis for hospitality at the Univ. of Crete. C.C. thanks the Theory Group at the University of Zurich at Irchel for hospitality during the last stages of this work.

A. Collinear expansion

The collinear expansion of the internal loop momentum k allows to identify the light cone operators appearing in the process at leading twist. We recall at this point that the analysis of the hand-bag contribution is carried out exactly as in the electromagnetic case.

To perform the collinear expansion and isolate the light-cone correlators of DVNS from the hand-bag contribution we use the relation

$$\int \frac{d\lambda\ dx}{2\pi} e^{i\lambda(x-k\cdot n)} = 1 \tag{A.1}$$

inside the expression of $T^{\mu\nu}$ in order to obtain

$$\begin{aligned} T^{\mu\nu} = & - \int \frac{d^4k}{(2\pi)^4} \int \frac{d\lambda\ dx}{2\pi} e^{i\lambda(x-k\cdot n)} \times \\ & \times \operatorname{tr}\left\{ \left[\gamma^\nu \frac{i}{\not{k} - \alpha\Delta + \not{q}_1 + i\epsilon}\gamma^\mu + \gamma^\mu \frac{i}{\not{k} + (1-\alpha)\not{\Delta} - \not{q}_1 + i\epsilon}\gamma^\nu \right] \underline{M}(k) \right\} \end{aligned}$$

and therefore

$$T^{\mu\nu} = -\int \frac{dk\cdot n\ dk\cdot\tilde{n}\ dk_\perp^2}{(2\pi)^4}\int\frac{d\lambda\ dx}{2\pi}e^{i\lambda(x-k\cdot n)}\int d^4z\ e^{ik\cdot z}\ \times$$
$$\times\ \mathrm{tr}\left\{\left[\gamma^\nu\frac{i}{\not{k}-\alpha\not{\Delta}+\not{q}_1+i\epsilon}\gamma^\mu+\gamma^\mu\frac{i}{\not{k}+(1-\alpha)\not{\Delta}-\not{q}_1+i\epsilon}\gamma^\nu\right]\cdot\right.$$
$$\left.\cdot\ \langle P'|\overline{\psi}(-\alpha z)\psi((1-\alpha)z)|P\rangle\right\}.$$

Keeping the leading terms for the loop momenta

$$k^\mu-\alpha\Delta^\mu+q_1^\mu = \tilde{n}^\mu\,(k\cdot n+2\alpha\xi-2\xi)+n^\mu\left(k\cdot\tilde{n}-\alpha\xi\overline{M}^2+\frac{Q^2}{4\xi}\right)$$
$$k^\mu+(1-\alpha)\Delta^\mu-q_1^\mu = \tilde{n}^\mu(k\cdot n-2(1-\alpha)\xi+2\xi)+n^\mu\left(k\cdot\tilde{n}+2(1-\alpha)\xi\overline{M}^2-\frac{Q^2}{4\xi}\right)$$

we thus obtain

$$T^{\mu\nu} = -\int\frac{d(k\cdot n)\ d(k\cdot\tilde{n})\ dk_\perp^2}{(2\pi)^4}\int\frac{d\lambda\ dx}{2\pi}e^{i\lambda(x-k\cdot n)}\int d^4z\ e^{ik\cdot z}\ \times$$
$$\times\ \mathrm{tr}\left\{\left[\gamma^\nu\frac{\not{\tilde{n}}}{2\left(k\cdot\tilde{n}-\alpha\xi\overline{M}^2+\frac{Q^2}{4\xi}\right)}\gamma^\mu+\gamma^\mu\frac{\not{\tilde{n}}}{2\left(k\cdot\tilde{n}+(1-\alpha)\xi\overline{M}^2-\frac{Q^2}{4\xi}\right)}\gamma^\nu+\right.\right.$$
$$\left.+\ \gamma^\nu\frac{\not{n}}{2(k\cdot n+2\alpha\xi-2\xi)}\gamma^\mu+\gamma^\mu\frac{\not{n}}{2(k\cdot n-2(1-\alpha)\xi+2\xi)}\gamma^\nu\right]\cdot$$
$$\left.\cdot\ \langle P'|\overline{\psi}(-\alpha z)\psi((1-\alpha)z)|P\rangle\right\}.$$

We expand

$$k\cdot z = (k\cdot n)\ (\tilde{n}\cdot z)+(k\cdot\tilde{n})\ (n\cdot z)-\vec{k}_\perp\cdot\vec{z}_\perp$$

and choose $\alpha = 1/2$. These expansions are introduced in eq. 3.16 and after some manipulations the tensor T now becomes

$$T^{\mu\nu}|_{\alpha=1/2} = -\int\frac{d(k\cdot n)\ d(k\cdot\tilde{n})\ dk_\perp^2}{(2\pi)^4}\int\frac{d\lambda\ dx}{2\pi}e^{i\lambda(x-k\cdot n)}\int d^4z\ e^{ik\cdot z}\ \times$$
$$\times\ \mathrm{tr}\left\{\left[\gamma^\nu\frac{\not{\tilde{n}}}{2\left(k\cdot\tilde{n}-\frac{\alpha}{2}\xi\overline{M}^2+\frac{Q^2}{2\xi}\right)}\gamma^\mu+\gamma^\mu\frac{\not{\tilde{n}}}{2\left(k\cdot\tilde{n}+(1-\alpha)\xi\overline{M}^2-\frac{Q^2}{4\xi}\right)}\gamma^\nu+\right.\right.$$
$$\left.+\ \gamma^\nu\frac{\not{n}}{2\left(k\cdot n+2\alpha\xi-2\xi\right)}\gamma^\mu+\gamma^\mu\frac{\not{n}}{2\left(k\cdot n-2(1-\alpha)\xi+2\xi\right)}\gamma^\nu\right]\cdot$$
$$\left.\cdot\ \langle P'|\overline{\psi}(-\alpha z)\psi((1-\alpha)z)|P\rangle\right\}.$$

We also recall that the expansion of the matrix element $\underline{M}(k)$ proceeds also in this case as in the electromagnetic case

$$\underline{M}_{ab}^{(i)}(k) = \int d^4 y e^{ik\cdot y} \langle P' | \overline{\psi}_a^{(i)}(-\alpha y) \psi_b^{(i)}((1-\alpha)y) | P \rangle = A_1 \not{\bar{n}} \;\; + A_2 \gamma_5 \not{\bar{n}} \;\; + \cdots . \qquad \text{(A.2)}$$

where the ellipses refer to terms which are of higher twist or disappear in the trace of the diagram.

B. Form factors parameterizations

The last ingredients needed in the construction of the input distribution functions are the form factors F_1^i and F_2^i. From experimental measurements we know, by a dipole parametrization in the small Δ^2 region, that

$$G_E^p(\Delta^2) = (1+\kappa_p)^{-1} G_M^p(\Delta^2) = \kappa_n^{-1} G_M^n(\Delta^2) = \left(1 - \frac{\Delta^2}{m_V^2}\right)^{-2}, \qquad G_E^n(\Delta^2) = 0\,, \quad \text{(B.1)}$$

where the electric, $G_E^i(\Delta^2) = F_1^i(\Delta^2) + \frac{\Delta^2}{4M^2} F_2^i(\Delta^2)$, and magnetic form factors $G_M^i(\Delta^2) = F_1^i(\Delta^2) + F_2^i(\Delta^2)$ are usually parametrized in terms of a cutoff mass $m_V = 0.84\,\text{GeV}$. For non-polarized GPD's the valence u and d quark form factors in the proton can be easily extracted from $F_I^{\binom{p}{n}} = 2\binom{Q_u}{Q_d} F_I^u + \binom{Q_d}{Q_u} F_I^d$ and given exclicitely by

$$2F_I^u(\Delta^2) = 2F_I^p(\Delta^2) + F_I^n(\Delta^2)\,, \qquad F_I^d(\Delta^2) = F_I^p(\Delta^2) + 2F_I^n(\Delta^2)\,, \quad \text{for } I = 1,2\,. \quad \text{(B.2)}$$

This exploits the fact that proton and neutron form an iso-spin doublet.

At the scale $m_A = 0.9\,\text{GeV}$ one can get

$$G_1^i(\Delta^2) = \left(1 - \frac{\Delta^2}{m_A^2}\right)^{-2} \qquad \text{(B.3)}$$

for the valence quarks. For the form factors F we obtain

$$\begin{aligned}
F_1^u &= -\frac{A\Delta^2}{M^2(1-B\Delta^2)^2\left(-1+\frac{\Delta^2}{4M^2}\right)} + \frac{1 - \frac{C\Delta^2}{M^2\left(1-\frac{\Delta^2}{4M^2}\right)}}{(1-B\Delta^2)^2}\,, \\
F_2^u &= \frac{D}{(1-B\Delta^2)^2\left(1-\frac{\Delta^2}{4M^2}\right)}\,, \\
F_1^d &= -\frac{E\Delta^2}{M^2(1-B\Delta^2)^2\left(-1+\frac{\Delta^2}{4M^2}\right)} + \frac{1 - \frac{C\Delta^2}{M^2\left(1-\frac{\Delta^2}{4M^2}\right)}}{(1-B\Delta^2)^2}\,, \\
F_2^d &= \frac{F}{(1-B\Delta^2)^2\left(1-\frac{\Delta^2}{4M^2}\right)}\,, \qquad \text{(B.4)}
\end{aligned}$$

where

$$\begin{aligned}
A &= 0.238 \qquad B = 1.417 \qquad C = 0.447\,, \\
D &= 0.835 \qquad E = 0.477 \qquad F = 0.120\,. \qquad \text{(B.5)}
\end{aligned}$$

C. Principle value prescription

In this section we illustrate an analytical computation of the integrals by discretization, using finite elements method. We want to approximate with high numerical accuracy integrals of the form

$$P.V. \int_{-1}^{1} \frac{H(z)dz}{z-\xi} = \int_{-1}^{\xi} dz \frac{H(z)-H(\xi)}{z-\xi} + \int_{\xi}^{1} dz \frac{H(z)-H(\xi)}{z-\xi} + H(\xi) \ln \left| \frac{\xi-1}{\xi+1} \right| . \quad \text{(C.1)}$$

For this purpose we start by choosing a grid on the interval $(-1 = x_0, \ldots, x_{n+1} = \xi)$ and define

$$J_1 = \int_{-1}^{\xi} dz \frac{H(z)-H(\xi)}{z-\xi} = \sum_{j=0}^{n} \int_{x_j}^{x_{j+1}} dx \frac{H(x)-H(\xi)}{x-\xi} . \quad \text{(C.2)}$$

Performing a simple linear interpolation we get

$$\begin{aligned} J_1 = & \sum_{j=0}^{n-1} \int_{x_j}^{x_{j+1}} \left\{ H(x_j) \left[\frac{x_{j+1}-x}{x_{j+1}-x_j} \right] + H(x_{j+1}) \left[\frac{x-x_j}{x_{j+1}-x_j} \right] \right\} \frac{dx}{x-\xi} + \\ & + \int_{x_n}^{\xi} \left\{ H(x_n) \left[\frac{\xi - x}{\xi - x_n} \right] + H(\xi) \left[\frac{x-x_n}{\xi-x_n} \right] \right\} \frac{dx}{x-\xi} - \int_{-1}^{\xi} dx \frac{H(\xi)}{x-\xi} . \end{aligned} \quad \text{(C.3)}$$

After the integration we are left with

$$\begin{aligned} J_1 = & \sum_{j=0}^{n-1} H(x_j) \left[-1 + \left(\frac{x_{j+1}-\xi}{x_{j+1}-x_j} \right) \ln \left| \frac{x_{j+1}-\xi}{x_j-\xi} \right| \right] + \\ & + \sum_{j=0}^{n-1} H(x_{j+1}) \left[1 + \left(\frac{\xi - x_j}{x_{j+1}-x_j} \right) \ln \left| \frac{x_{j+1}-\xi}{x_j-\xi} \right| \right] - \\ & - \sum_{j=0}^{n-1} H(\xi) \ln \left| \frac{x_{j+1}-\xi}{x_j-\xi} \right| - H(x_n) + H(\xi) . \end{aligned} \quad \text{(C.4)}$$

Now, moving to the integral in the interval $(\xi, 1)$, we introduce a similar grid of equally spaced points $(\xi = y_0, \ldots, y_{n+1} = 1)$ and define the integral

$$J_2 = \int_{\xi}^{1} dz \frac{H(z)-H(\xi)}{z-\xi} = \sum_{j=0}^{n} \int_{y_j}^{y_{j+1}} dy \frac{H(y)-H(\xi)}{y-\xi} . \quad \text{(C.5)}$$

As above, after isolating the singularity we obtain

$$\begin{aligned} J_2 = & \sum_{j=1}^{n} \int_{y_j}^{y_{j+1}} \left\{ H(y_j) \left[1 - \frac{y-y_j}{y_{j+1}-y_j} \right] + H(y_{j+1}) \left[\frac{y-y_j}{y_{j+1}-y_j} \right] \right\} \frac{dy}{y-\xi} + \\ & + H(y_1) + H(\xi) \int_{\xi}^{y_1} \left[\frac{y_1 - y}{y_1 - \xi} \right] dy - \int_{\xi}^{1} dy \frac{H(\xi)}{y-\xi} . \end{aligned} \quad \text{(C.6)}$$

Again, performing the integrations we obtain

$$
\begin{aligned}
J_2 = & \sum_{j=1}^{n} H(y_j)\left[-1+\left(\frac{y_{j+1}-\xi}{y_{j+1}-y_j}\right)\ln\left|\frac{y_{j+1}-\xi}{y_j-\xi}\right|\right]+ \\
& +\sum_{j=1}^{n} H(y_{j+1})\left[1+\left(\frac{\xi-y_j}{y_{j+1}-y_j}\right)\ln\left|\frac{y_{j+1}-\xi}{y_j-\xi}\right|\right]- \\
& -\sum_{j=1}^{n} H(\xi)\ln\left|\frac{y_{j+1}-\xi}{y_j-\xi}\right| + H(y_1) - H(\xi)\,.
\end{aligned} \tag{C.7}
$$

Collecting our results, at the end we obtain

$$
P.V.\int_{-1}^{1}\frac{H(z)dz}{z-\xi} = J_1 + J_2 + H(\xi)\ln\left|\frac{\xi-1}{\xi+1}\right|. \tag{C.8}
$$

We can use the same strategy for the integrals of "+" type defined as follows

$$
P.V.\int_{-1}^{1}\frac{H(z)dz}{z+\xi} = \int_{-1}^{-\xi} dz\frac{H(z)-H(-\xi)}{z+\xi} + \int_{-\xi}^{1} dz\frac{H(z)-H(-\xi)}{z+\xi} + H(-\xi)\ln\left|\frac{\xi+1}{\xi-1}\right|. \tag{C.9}
$$

This time we call our final integrals X_1 and X_2. They are given by the expressions

$$
\begin{aligned}
X_1 = & \sum_{j=0}^{n-1} H(x_j)\left[-1+\left(\frac{x_{j+1}+\xi}{x_{j+1}-x_j}\right)\ln\left|\frac{x_{j+1}+\xi}{x_j+\xi}\right|\right]+ \\
& +\sum_{j=0}^{n-1} H(x_{j+1})\left[1+\left(\frac{-\xi-x_j}{x_{j+1}-x_j}\right)\ln\left|\frac{x_{j+1}+\xi}{x_j+\xi}\right|\right]- \\
& -\sum_{j=0}^{n-1} H(-\xi)\ln\left|\frac{x_{j+1}+\xi}{x_j+\xi}\right| - H(x_n) + H(-\xi)\,,
\end{aligned} \tag{C.10}
$$

with a discretization supported in the $(-1 = x_0, \ldots, x_{n+1} = \xi)$ grid, and

$$
\begin{aligned}
X_2 = & \sum_{j=1}^{n} H(y_j)\left[-1+\left(\frac{y_{j+1}+\xi}{y_{j+1}-y_j}\right)\ln\left|\frac{y_{j+1}+\xi}{y_j+\xi}\right|\right]+ \\
& +\sum_{j=1}^{n} H(y_{j+1})\left[1+\left(\frac{-\xi-y_j}{y_{j+1}-y_j}\right)\ln\left|\frac{y_{j+1}+\xi}{y_j+\xi}\right|\right]- \\
& -\sum_{j=1}^{n} H(-\xi)\ln\left|\frac{y_{j+1}+\xi}{y_j+\xi}\right| + H(y_1) - H(-\xi)\,,
\end{aligned} \tag{C.11}
$$

on the $(-\xi = y_0, \ldots, y_{n+1} = 1)$ grid. As a final result for the "+" integral we get

$$
P.V.\int_{-1}^{1}\frac{H(z)dz}{z+\xi} = X_1 + X_2 + H(-\xi)\ln\left|\frac{\xi+1}{\xi-1}\right|. \tag{C.12}
$$

D. Expressions of the squared amplitude

In this section we will present the full expression of the functions A_1 and A_2 which appear in the squared amplitude

$$\begin{aligned}
A_1(z,z'x,t,Q^2) \;=\; \tilde{g}^4 Q^2 \Big[& 4g_d^2[\tilde{E}'_d(4\tilde{H}_d M^2+\tilde{E}_d t)x^2+4\tilde{H}'_d M^2(4\tilde{H}_d(x-1)+\tilde{E}_d x^2)]+\\
& +4g_d g_u\Big[(4\tilde{E}'_u\tilde{H}_d M^2++4\tilde{E}'_d\tilde{H}_u M^2+\tilde{E}'_u\tilde{E}_d t+\tilde{E}'_d\tilde{E}_u t)x^2\\
& \qquad +4\tilde{H}'_u M^2(4\tilde{H}_d(x-1)+\tilde{E}_d x^2)+\\
& \qquad +4\tilde{H}'_d M^2(4\tilde{H}_u(x-1)+\tilde{E}_u x^2)\Big]+\\
& +D_v U_v g_d g_u\Big[4E'_u E_d t+4E'_d E_u t-4E'_u E_d t x-4E'_d E_u t x+\\
& \qquad +4E'_u E_d M^2 x^2+4E'_d E_u M^2 x^2+4E'_u H_d M^2 x^2+\\
& \qquad +4E'_d H_u M^2 x^2+E'_u E_d t x^2+E'_d E_u t x^2+\\
& \qquad +4H'_u M^2(4H_d(x-1)+E_d x^2)+\\
& \qquad +4H'_d M^2(4H_u(x-1)+E_u x^2)\Big]+\\
& +g_u^2\Big[4E'_u E_u t U_v^2-4E'_u E_u t U_v^2 x+16\tilde{E}'_u\tilde{H}_u M^2 x^2+4\tilde{E}'_u\tilde{E}_u t x^2+\\
& \qquad +4E'_u E_u M^2 U_v^2 x^2+4E'_u H_u M^2 U_v^2 x^2+E'_u E_u t U_v^2 x^2+\\
& \qquad +16\tilde{H}'_u M^2(4\tilde{H}_u(x-1)+\tilde{E}_u x^2)+\\
& +4H'_u M^2 U_v^2(4H_u(x-1)+E_u x^2)\Big]+\\
& +D_v^2 g_d^2\Big[4H'_d M^2(4H_d(x-1)+E_d x^2)+\\
& \qquad +E'_d(4H_d M^2 x^2+E_d(t\,(x-2)^2+4M^2x^2))]\Big]
\end{aligned} \tag{D.1}$$

and for $A_2(z,z',x,t)$ we get a similar result

$$\begin{aligned}
A_2(z,z',x,t,Q^2) \;=\; 4\tilde{g}^4 Q^2\Big[& g_d g_u\Big[4E'_u E_d t+4E'_d E_u t-16D_v\tilde{H}'_u\tilde{H}_d M^2 U_v-16D_v\tilde{H}'_d\tilde{H}_u M^2 U_v-\\
& \qquad -4E'_u E_d t x-4E'_d E_u t x+16D_v\tilde{H}_u\tilde{H}_d M^2 U_v x+\\
& \qquad +16D_v\tilde{H}'_d\tilde{H}_u M^2 U_v x+4E'_u E_d M^2 x^2+4E'_d E_u M^2 x^2+\\
& \qquad +4E'_u H_d M^2 x^2+4E'_d H_u M^2 x^2+E'_u E_d t x^2+E'_d E_u t x^2+\\
& \qquad +4D_v\tilde{E}_u\tilde{H}'_d M^2 U_v x^2+4D_v\tilde{E}_d\tilde{H}'_u M^2 U_v x^2+\\
& \qquad +4D_v\tilde{E}'_u\tilde{H}_d M^2 U_v x^2+4D_v\tilde{E}'_d\tilde{H}_u M^2 U_v x^2+D_v\tilde{E}'_u\tilde{E}_d t U_v x^2+\\
& \qquad +D_v\tilde{E}'_d\tilde{E}_u t U_v x^2+4H'_u M^2(4H_d(x-1)+E_d x^2)+\\
& \qquad +4H'_d M^2(4H_u(x-1)+E_u x^2)\Big]+\\
& +g_d^2\Big[4H'_d M^2(4H_d(x-1)+E_d x^2)+D_v^2(\tilde{E}'_d(4\tilde{H}_d M^2+\tilde{E}_d t)x^2+\\
& \qquad +4\tilde{H}'_d M^2(4\tilde{H}_d(x-1)+\tilde{E}_d x^2))+\\
& \qquad +E'_d(4H_d M^2 x^2+E_d(t(x-2)^2+4M^2x^2))\Big]+\\
& +g_u^2[4H'_u M^2(4H_u(x-1)+E_u x^2)+\\
& \qquad +U_v^2(\tilde{E}'_u(4\tilde{H}_u M^2+\tilde{E}_u t)x^2+4\tilde{H}'_u M^2(4\tilde{H}_u(x-1)+\tilde{E}_u x^2))+\\
& \qquad +E'_u(4H_u M^2 x^2+E_u(t(x-2)^2+4M^2x^2))\Big]\Big]\,.
\end{aligned} \tag{D.2}$$

JHEP02(2005)038

References

[1] J.W.F. Valle, *Brief neutrino physics update*, hep-ph/0310125;
S. Pakvasa and J.W.F. Valle, *Neutrino properties before and after kamland*, *Proc. Indian Natl. Sci. Acad.* **70A** (2004) 189–222 [hep-ph/0301061].

[2] MINOS collaboration, J. Hurheim, *Status of the MINOS experiment and review of long-baseline neutrino oscillation experiments in Europe and North America* in *31st ICHEP 2002*, Amsterdam, Jul 2002.

[3] M.V. Diwan et al., *Very long baseline neutrino oscillation experiments for precise measurements of mixing parameters and CP-violating effects*, *Phys. Rev.* **D 68** (2003) 012002 [hep-ph/0303081];
W.T. Weng et al., *The neutrino superbeam from the Ags*, *J. Phys.* **G29** (2003) 1735;
W. Marciano, *Very-long baseline neutrino oscillations and precision measurements*, talk at the *KITP conference. Neutrinos: data, cosmos, and planck scale*, Mar 3-7, 2003.

[4] M.L. Mangano et al., *Physics at the front-end of a neutrino factory: a quantitative appraisal*, hep-ph/0105155.

[5] G. Sterman and P. Stoler, *Hadronic form-factors and perturbative QCD*, *Ann. Rev. Nucl. Part. Sci.* **47** (1997) 193.

[6] X.-D. Ji, *Deeply-virtual compton scattering*, *Phys. Rev.* **D 55** (1997) 7114 [hep-ph/9609381].

[7] A.V. Radyushkin, *Nonforward parton distributions*, *Phys. Rev.* **D 56** (1997) 5524 [hep-ph/9704207].

[8] A.V. Radyushkin, *Double distributions and evolution equations*, *Phys. Rev.* **D 59** (1999) 014030 [hep-ph/9805342].

[9] J. Blumlein, J. Eilers, B. Geyer and D. Robaschik, *On the structure of the virtual compton amplitude with additional final state meson in the extended Bjorken region*, *Phys. Rev.* **D 65** (2002) 054029 [hep-ph/0108095].

[10] A.V. Radyushkin and C. Weiss, *Dvcs amplitude at tree level: transversality, twist-3 and factorization*, *Phys. Rev.* **D 63** (2001) 114012 [hep-ph/0010296].

[11] J. Blumlein and N. Kochelev, *On the twist 2 and twist 3 contributions to the spin-dependent electroweak structure functions*, *Nucl. Phys.* **B 498** (1997) 285 [hep-ph/9612318].

[12] M. Penttinen, M.V. Polyakov, A.G. Shuvaev and M. Strikman, *DVCS amplitude in the parton model*, *Phys. Lett.* **B 491** (2000) 96 [hep-ph/0006321].

[13] J.C. Collins and A. Freund, *Proof of factorization for deeply virtual compton scattering in QCD*, *Phys. Rev.* **D 59** (1999) 074009 [hep-ph/9801262].

[14] X. Ji, *J. Phys.* **G24** (1998) 1181.

[15] A.V. Belitsky, D. Muller, L. Niedermeier and A. Schafer, *Leading twist asymmetries in deeply virtual compton scattering*, *Nucl. Phys.* **B 593** (2001) 289 [hep-ph/0004059].

[16] I.V. Musatov and A.V. Radyushkin, *Evolution and models for skewed parton distributions*, *Phys. Rev.* **D 61** (2000) 074027 [hep-ph/9905376].

[17] K.J. Golec-Biernat and A.D. Martin, *Off-diagonal parton distributions and their evolution*, *Phys. Rev.* **D 59** (1999) 014029 [hep-ph/9807497].

[18] A. Freund and M. McDermott, *A detailed next-to-leading order QCD analysis of deeply virtual compton scattering observables*, *Eur. Phys. J.* **C 23** (2002) 651.

[19] K. Golec-Biernat, A.D. Martin and M.G. Ryskin, *Initial conditions and evolution of off-diagonal distributions*, *Nucl. Phys.* **79** *(Proc. Suppl.)* (1999) 365 [hep-ph/9905517].

[20] A. Freund, M. McDermott and M. Strikman, *Modelling generalized parton distributions to describe deeply virtual compton scattering data*, *Phys. Rev.* **D 67** (2003) 036001 [hep-ph/0208160].

[21] M. Vanderhaeghen, P.A.M. Guichon and M. Guidal, *Deeply virtual electroproduction of photons and mesons on the nucleon: leading order amplitudes and power corrections*, *Phys. Rev.* **D 60** (1999) 094017 [hep-ph/9905372].

[22] M. Gluck, E. Reya and A. Vogt, *Dynamical parton distributions revisited*, *Eur. Phys. J.* **C 5** (1998) 461 [hep-ph/9806404].

[23] X.-d. Ji, *Generalized parton distributions and the spin structure of the nucleon*, *Nucl. Phys.* **119** *(Proc. Suppl.)* (2003) 41 [hep-lat/0211016].

[24] L. Mankiewicz, G. Piller and A. Radyushkin, *Hard exclusive electroproduction of pions*, *Eur. Phys. J.* **C 10** (1999) 307 [hep-ph/9812467].

[25] L.L. Frankfurt, P.V. Pobylitsa, M.V. Polyakov and M. Strikman, *Hard exclusive pseudoscalar meson electroproduction and spin structure of a nucleon*, *Phys. Rev.* **D 60** (1999) 014010 [hep-ph/9901429].

[26] L. Mankiewicz, G. Piller and T. Weigl, *Hard exclusive meson production and nonforward parton distributions*, *Eur. Phys. J.* **C 5** (1998) 119.

[27] A. Freund and M. McDermott, *A next-to-leading order QCD analysis of deeply virtual compton scattering amplitudes*, *Phys. Rev.* **D 65** (2002) 074008.

[28] E.A. Paschos and A.V. Kartavtsev, *Coherent neutrino nucleus scattering*, hep-ph/0309148.

[29] C. Corianò, M. Guzzi and J.D. Vergados, in preparation.